

RESEARCH ARTICLE

Broad-spectrum antiviral activity of *Spatholobus suberectus* Dunn against SARS-CoV-2, SARS-CoV-1, H5N1, and other enveloped viruses

Qingqing Liu^{1,2} | Ka-Yi Kwan³ | Tianyu Cao^{3,4} | Bingpeng Yan⁵ |
Kumar Ganesan¹  | Lei Jia^{1,2} | Feng Zhang^{1,2} | Chunyu Lim³ | Yaobin Wu⁶ |
Yibin Feng¹  | Zhiwei Chen^{3,5}  | Li Liu^{3,5} | Jianping Chen^{1,2} 

¹School of Chinese Medicine, Li Ka Shing Faculty of Medicine, The University of Hong Kong, Hong Kong, China

²Shenzhen Institute of Research and Innovation, University of Hong Kong, Shenzhen, China

³AIDS Institute, State Key Laboratory of Infectious Diseases, Li Ka Shing Faculty of Medicine, The University of Hong Kong, Hong Kong, China

⁴Department of Immunology and Department of Dermatology, Tangdu Hospital, Fourth Military Medical University, Xi'an, China

⁵Department of Microbiology, Li Ka Shing Faculty of Medicine, The University of Hong Kong, Hong Kong, China

⁶Guangdong Engineering Research Center for Translation of Medical 3D Printing Application, Guangdong Provincial Key Laboratory of Medical Biomechanics, Department of Human Anatomy, School of Basic Medical Sciences, Southern Medical University, Guangzhou, China

Correspondence

Zhiwei Chen and Li Liu, AIDS Institute, State Key Laboratory of Infectious Diseases, Department of Microbiology, Li Ka Shing Faculty of Medicine, The University of Hong Kong, Hong Kong, China.
Email: zchenai@hku.hk (Z.C.) and
Email: liuli71@hku.hk (L.L.)

Jianping Chen, School of Chinese Medicine, Li Ka Shing Faculty of Medicine, The University of Hong Kong, Hong Kong, China.
Email: abchen@hku.hk (J.C.)

Funding information

Guangxi Science and Technology Key Research and Development Program, Grant/Award Number: AB16450012

Abstract

The current COVID-19 pandemic caused by SARS-Cov-2 is responsible for more than 6 million deaths globally. The development of broad-spectrum and cost-effective antivirals is urgently needed. Medicinal plants are renowned as a complementary approach in which antiviral natural products have been established as safe and effective drugs. Here, we report that the percolation extract of *Spatholobus suberectus* Dunn (SSP) is a broad-spectrum viral entry inhibitor against SARS-CoV-1/2 and other enveloped viruses. The viral inhibitory activities of the SSP were evaluated by using pseudotyped SARS-CoV-1 and 2, HIV-1_{ADA} and HXB2, and H5N1. SSP effectively inhibited viral entry and with EC₅₀ values ranging from 3.6 to 5.1 µg/ml. Pre-treatment of pseudovirus or target cells with SSP showed consistent inhibitory activities with the respective EC₅₀ value of 2.3 or 2.1 µg/ml. SSP blocked both SARS-CoV-2 spike glycoprotein and the host ACE2 receptor. *In vivo* studies indicated that there was no abnormal toxicity and behavior in long-term SSP treatment. Based on these findings, we concluded that SSP has the potential to be developed as a drug candidate for preventing and treating COVID-19 and other emerging enveloped viruses.

KEYWORDS

antivirals, H5N1, HIV-1, SARS-CoVs, *Spatholobus suberectus* Dunn

1 | INTRODUCTION

The Coronavirus disease 2019 (COVID-19) pandemic is a significant threat to global health caused by the severe acute respiratory syndrome coronavirus 2 (SARS-CoV-2) since December 2019 (Wu, Leung, & Leung, 2020). The COVID-19 pandemic has led to over 477 million laboratory-confirmed cases and about 6 million deaths worldwide. Although there has been limited data about the virus, present evidence shows that the public gets severe illnesses from COVID-19 irrespective of their gender, age, ethnicity, and health status (Hu, Guo, Zhou, & Shi, 2021). Being greatly transmissible, this novel COVID-19 has spread fast globally and overwhelmingly surpassed severe acute respiratory syndrome (SARS) and the Middle East respiratory syndrome (MERS) in terms of both the number of infected persons and the range of epidemic areas (Zhu et al., 2020). No effective treatment for this disease was substantiated, thus the morbidity and death rate would be always greater than common respiratory infection. Hence, it requires immediate clinical interventions and great efforts are needed to find effective drugs.

The epidemic outbreaks caused by the emerging and re-emerging viruses represent an extraordinary threat to global public health (Chan et al., 2020). Re-emerging viruses associated with emerging infectious diseases have been increasing nowadays and high mortality occurred especially when healthcare resources were overwhelmed (Dong, Du, & Gardner, 2020). As a novel beta coronavirus, SARS-CoV-2 shares 79% genome sequence character with SARS-CoV and 50% with MERS-CoV (Lu et al., 2020). In addition to SARS-CoV-2, other re-emerging viruses such as the influenza A virus (IAV), and the human immunodeficiency virus (HIV) are clinically important. The genome organization of SARS-CoV-2 shares homology with other beta coronaviruses. The viral replication cycle generally involves multiple steps, including viral entry, genome transcription and translation, virion assembly in the endoplasmic reticulum-Golgi intermediate compartment (ERGIC), and finally virion budding by exocytosis (Fehr & Perlman, 2015). The entry of CoVs and other viruses are initiated by viral receptor-binding domain (RBD) and subsequent membrane fusion, where the spike (S) proteins of CoVs or envelope (ENV) protein of other viruses and viral receptors expressed on target cells play critical roles (Matsuyama et al., 2020).

In the RBD of S protein, the amino acid similarity between SARS-CoV-2 and SARS-CoV is about 73%. The S protein present in SARS-CoV-2 plays as a viral antigen and is accountable for binding to the host receptor eliciting humoral and cell-mediated immune responses during infection. A specific genomic feature of SARS-CoV-2 is the insertion of four amino acid residues at the junction of subunits of the S glycoprotein (Andersen, Rambaut, Lipkin, Holmes, & Garry, 2020). This insertion creates a polybasic cleavage site, which permits effective cleavage by furin and other proteases (Coutard et al., 2020). A structural study suggested that the furin-cleavage site can reduce the stability of SARS-CoV-2 S glycoprotein and facilitate the conformational adaption that is essential for the binding of the RBD to its receptor (Wrobel et al., 2020). The binding of SARS-CoV-2 with

angiotensin-converting enzyme 2 (ACE2) enables virus entry into the host cells (Xu et al., 2020). Obstructing viral entry is one of the effective strategies to inhibit viral infection. Several studies have successfully targeted this mechanism for antiviral treatment. For instance, structurally distinctive novel fusion inhibitors FA-583 and FA-617 inhibit the fusion of IAV by blocking the low-pH-induced hemagglutinin (Lai et al., 2015). Similarly, Maraviroc (Tan et al., 2013), enfuvirtide (Ikeda, Tennyson, Walker, Harris, & McNaughton, 2019), and Ibalizumab (Blair, 2020) inhibit HIV entry by blocking viral receptor binding. Only limited antiviral drugs are licensed for clinical practice for these diseases (Zhou et al., 2021). The situation is further exacerbated by the potential development of drug-resistant mutants (Li et al., 2020; Weinreich et al., 2021). Hence, there is an urgent need to find broad-spectrum antiviral agents that are highly efficient and cost-effective to combat the current COVID-19 pandemic and emerging variants of related viruses.

Nowadays, structure-based drug design strategies have been implemented to explicate the antiviral activity of active constituents present in traditional medicinal plants. Recently, several natural products are recognized as adjuvant therapy for COVID-19 treatment, not only for direct antiviral therapy (Islam et al., 2020), but also as an immune enhancer (Shah et al., 2021). Notably, natural products/medical herbs also have potential therapeutic effects for COVID-19-related sequelae, including cardiovascular complications (Mohammadi Pour, Farzaei, Soleiman Dehkordi, Bishayee, & Asgary, 2021). *Spatholobus suberectus* Dunn (SS, Latin name: *Spatholobi caulis*) belongs to the Rosales, Leguminosae family, which is widely distributed in Yunnan, Guangxi, Guangdong, and Fujian provinces of China. Its dried vine stem is well-recognized as Ji Xue Teng in the Chinese Pharmacopoeia, which is widely used in Traditional Chinese Medicine to treat blood stasis syndrome, abnormal menstruation, blood deficiency, chlorosis, and rheumatism (Mei et al., 2019; Qin et al., 2019). SS contains various classes of bioactive rich compounds viz., proanthocyanidins (PACs), flavonoids, phenolic compounds, quinones, and saponins (Cheng, Wan et al., 2011; Yoon, Sung, Park, & Kim, 2004), which exhibits various pharmacological activities including, antiinflammatory, antioxidant, antiplatelet, anticancer, and antiviral activity, affecting hemagglutination and lipid regulation (Chen et al., 2004; Chen et al., 2016; Im et al., 2014; Lee et al., 2011; Wang et al., 2013). Earlier studies suggested that extract of SS have potent antiviral activities against hepatitis C virus (Chen et al., 2016), coxsackievirus B3 (Pang et al., 2011), and enteroviruses, including coxsackievirus B5, Poliovirus 1, Echovirus 9. and Echovirus 29 (Guo et al., 2006).

Hence, we aimed to investigate the broad-spectrum viral entry inhibitory activity and underlying mechanisms of SSP against SARS-CoV-2, SARS-CoV-1, HIV-1_{ADA}, HIV-1_{HXB2}, H5N1, and Indiana vesiculovirus. Further extraction and isolation of SSP were also performed to determine active constituents. In addition, *in vivo* studies and quality control assays were also performed to analyze the drug-likeness, and toxicity to ensure the safety and efficacy of SSP.

2 | MATERIALS AND METHODS

2.1 | Extraction of *Spatholobus suberectus* Dunn

Dried SS stems were purchased from KangMei Pharmaceutical Company Ltd (Guang Xi Province, China) and the plants were authenticated by inspectors in the School of Chinese Medicine, the University of Hong Kong, Hong Kong. Briefly, SS was ground into coarse powder and extracted using a percolating device with 10 times volume (v/w) of 60% ethanol. The extract was then concentrated by reduced pressure to obtain the percolation powder, named SSP. SSP was dissolved in dimethyl sulfoxide (DMSO) to reach a concentration of 40 mg/ml for future use. About 200 g SSP extract was weighed and dispersed evenly in an appropriate amount of water to obtain the aqueous solution, followed by extraction with equal volumes of petroleum ether (PE), ethyl acetate (EA), and n-butanol (n-BuOH) to obtain the following parts: 2 g petroleum ether part (SSP-PE), 12.8 g ethyl acetate part (SSP-EA), 8.2 g EA insoluble part (SSP-EAin), 62 g n-butanol part (SSP-n-BuOH) and 113 g water layer residue (SSP-W). Then the n-butanol part (SSP-n-BuOH) was subjected to macroporous resin columns for gradient elution ethanol-water to obtain fraction A ~ J (Figure 1).

The contents of PACs in SSP were determined by the vanillin-hydrochloric acid method (Data S1) with minor modification (Cheng, Fu, et al., 2011). UHPLC of SSP was performed by Ultimate 3,000 system (Thermo Fisher Scientific Inc., Waltham, Massachusetts, U.S.) with a diode array detector (DAD). Before injection, the samples were

filtrated through a 0.22 μm PTFE filter. An ACE Excel 2 C₁₈ column (100 mm \times 2.1 mm id, Scotland, UK) was used for the chromatographic separation, and the mobile phase was composed of acetonitrile (solvent A) and Milli-Q water with 0.1% formic acid (solvent B), using a gradient elution of 0 min 95% B, 3 min 92% B, 20 min 85% B, 26 min 70% B, 30 min, 40% B, 35 min 5% B, and keep at 5% B for five more minutes. The solvent flow rate was set as 0.4 ml/min, and the wavelength for analysis was conducted at 280 nm (Figure 2a). This method was validated and shown in Data S2.

2.2 | Identification of SSP by TLC

According to the Chinese Pharmacopoeia (version of the Year 2015), SSP was identified by thin-layer chromatography (TLC). Sonicated 2 g SSP with 40 ml of ethanol for 30 min. After filtration and rotary evaporation, dissolve the residue with 10 ml of water, and then extract using 10 ml of ethyl acetate. After removing the solvent, dissolve the residue with 1 ml of methanol to obtain the test solution. The control was prepared according to the same protocol. About 5–10 μl of the test and the control samples were drawn on the GF₂₅₄ thin-layer plate of silica gel, dichloromethane-acetone-methanol-formic acid (8:1.2:0.3:0.5) as the developing agent was used. The plate was then sprayed using 5% vanillin sulfuric acid solution and heated at 105°C until getting the clear spots. Based on the color spot on the chromatogram, the compounds of SSP were identified according to the corresponding position of the control (Figure 2b).

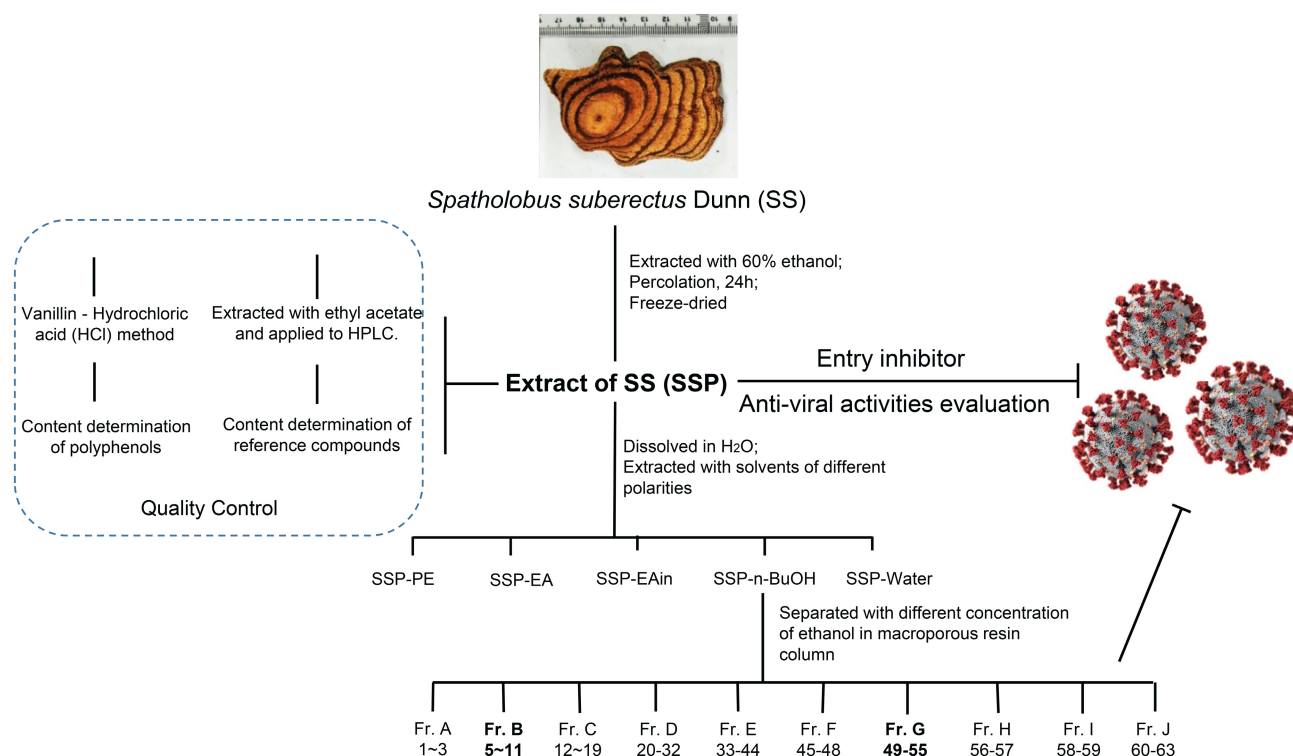


FIGURE 1 Flow chart of the study. Preparation and quality-controlled of SSP which is used to determine the broad-spectrum antiviral activity and its underlying mechanism. The powder SSP was further extracted to determine the effective active parts

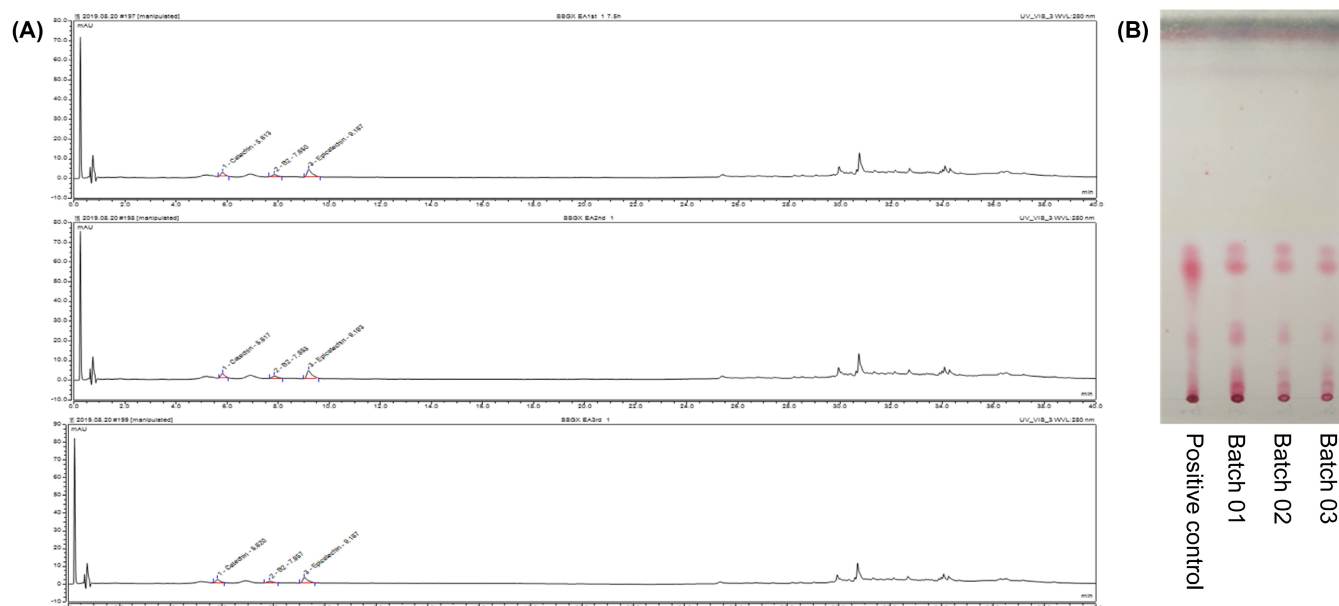


FIGURE 2 Representative pictures of SSP's quality control. (a) HPLC chromatogram of different batches of SSP after ethyl acetate processing. (b) TLC chromatogram of different batches of SSP and positive control of SS

2.3 | Cell culture

Highly sensitive and transferable cell lines, 293 T, TZM-bl, and MDCK, which were obtained from American Type Culture Collection (ATCC, MN, USA), and passage numbers were within 10 times. The cells were cultivated in Dulbecco's modified Eagle medium (DMEM, Gibco, Grand Island, NY, USA) with 10% inactivated fetal bovine serum (FBS, Gibco, Grand Island, NY, USA), 1% mixture of 100 units/ml penicillin, and 100 μ g/ml streptomycin (P/S, Sigma-Aldrich, St. Louis, MO, USA). HEK293T-ACE2 was cultivated in DMEM with 10% FBS, 1% P/S, and 1 μ g/ml puromycin (Sigma-Aldrich, St. Louis, MO, USA). GHOST (3)-CD4-CCR5/CXCR4 cell lines were cultivated in DMEM with 10% FBS, 1% P/S, and 100 μ g/ml hygromycin B, 500 μ g/ml G418, and 1 μ g/ml puromycin (Sigma-Aldrich, St. Louis, MO, USA).

2.4 | Pseudovirus generation

We inserted an optimized full-length S gene of SARS-CoV-2 (QHR63250) into the pVAX-1 vector, namely pVax-1-S-COVID19. The construction was confirmed by sequence analysis. Single-cycle luciferase SARS-CoV-2, SARS-CoV-1, HIV_{ADA}, HIV_{HXB2}, H5N1, and Vesicular stomatitis Indiana virus (VSV) pseudoviruses were constructed as previously described (Liu et al., 2007; Yi, Ba, Zhang, Ho, & Chen, 2005). Briefly, pseudoviruses were generated by co-transfection of 293 T cells with HIV-1 NL4-3 Δ Env Vpr Luciferase (pNL4-3.Luc.R-E-) (NIH AIDS Reagent Program, Cat #3418) and envelope protein from different strains of viruses (polyethyleneimine [PEI]; Polysciences Inc., Warrington, PA). Cell-free supernatant was collected 48 h post-transfection and frozen at -80°C . To determine the viral titer, around 10,000 HEK293T-ACE2

cells per well in 96-well plates were seeded in 10% FBS-containing media. Cells were infected with serially diluted SARS-CoV-2 pseudovirus in a final volume of 200 μ l. After 48 hr, infected cells were lysed to measure luciferase activity using a commercial kit (Promega, E1500, Madison, WI). The 50% tissue culture infective dose (TCID₅₀) was calculated using the "TCID" macro as described previously (Richards & Clapham, 2006).

2.5 | The antiviral assays

The inhibitory activities of the SSP against viruses are evaluated as previously described (Liu et al., 2007; Lu et al., 2012). Briefly, serially diluted SSP was tested against 100TCID₅₀ viral infection. HEK293T-ACE2 were used for SARS-CoV-1/2; MDCK was used for H5N1; GHOST (3)-CD4-CCR5/CXCR4 were used for HIV_{ADA} and HIV_{HXB2} infection. On day three, the viral infection was determined by measuring the reporter luciferase activity in target cells post-infection using commercially available kits (Promega, Wisconsin, USA). Antiviral data are reported as the concentration of drugs required to inhibit viral replication by 50% (EC₅₀).

2.6 | The cytotoxicity assays

Cells were incubated in the presence or absence of serially diluted SSP at 37°C in 5% CO₂ for 48 hours. The viability of the cells was then measured using the CellTiter-Glo[®] Luminescent Cell Viability Assay kit (Promega, Wisconsin, USA). The cytotoxicity was generated according to the sample concentrations and luminescent values. The result was analyzed based on the formula:

$$\% \text{cell viability} = 100 \times \left(1 - \frac{\text{Luminescent value of the sample}}{\text{Luminescent value of cells alone}} \right)$$

2.7 | Flow cytometry analysis

This was performed to detect the binding between SARS-CoV-2 RBD and ACE2. Briefly, SSP pretreated (100 $\mu\text{g/ml}$ or 50 $\mu\text{g/ml}$) HEK293T-ACE2 cells were incubated with PD1-Tagged SARS-CoV-2 RBD or goat anti-ACE2 antibody (10 $\mu\text{g/ml}$) (R&D systems, MN, USA) for 30 min on ice. After three washes, the cells were incubated with PE anti-human PD1 antibody (biolegend, CA, USA) or APC anti-goat IgG antibody for 30 min on ice. The mixture was analyzed by flow cytometry.

2.8 | UPLC-DAD analysis and UPLC-ESI-QTOF-MS/MSn detection

The UPLC-DAD analysis was conducted with the same instrument as described above, but the gradient elution (name as "SSP isolation method") was different as follows: 0 min, 95% B; 1 min, 95% B; 3 min, 87% B; 9 min, 87% B; 11 min, 77% B; 21 min, 77% B; 23 min, 60% B; 33 min, 60% B; 35 min, 5% B; 40 min, 5% B. UV wavelength for analysis was also set at 280 nm. UPLC-QTOF-MS analysis was conducted using an Acquity UPLC system coupled to a Synapt G2-Si High-Definition Mass Spectrometry system (HDMS, Waters Corp., Milford, MA, USA) with MassLynx software version 4.1 (Waters Corp., Milford, MA, USA) software for data acquisition and analysis. After filtration through a 0.22 μm PTFE filter, SSP solution (10 mg/ml in methanol) was injected into the UPLC system (same as "SSP isolation method") for chromatography separation and further ESI source for mass detection. The mass spectra were recorded from m/z 150 to 1,200 in negative-ion mode. The other instrumental parameters of the ESI-MS analysis were as follows: capillary voltage, 3,500 V; nebulizer gas (N_2), 10 psi; and source temperature, 350°C.

2.9 | Thiolysis and UPLC analysis

Thiolysis and UHPLC analysis were performed according to the method of Li et al. (2015) with slight changes, with details as follows: (a) Prepare the sample solution of different fractions (dissolve 20 mg/ml in methanol), draw 100 μl solution into a sealable glass test tube; (b) Prepare the methanol solution with concentrated HCl (3.3% v/v), absorb 100 μl into the tube; (c) Prepare a 5% v/v toluene-alpha-thiol (Sigma-Aldrich, St. Louis, MO, USA) solution in methanol, absorb 200 μl into the tube; (d) Close tightly and incubate in a circulating water bath at 40°C for 30 min; (e) After the reaction, the sample solutions are filtrated through a 0.22 μm PTFE filter and injected into the UPLC-DAD system. The mobile phase consisted of acetonitrile (solvent A) and Milli-Q water (solvent B). The method was 0 min, 95% B;

10 min, 85% B; 15 min, 67% B; 22.5 min, 67% B; 27.5 min, 10% B; 32.5 min, 10% B. The sample injection volume was 5 μl , the flow rate was 0.4 ml/min, and the 280 nm UV absorption was chosen for analysis. The mDP values were calculated by using this equation (Li et al., 2015): $\text{mDP} = (\text{total area of benzyl-thioethers})/(\text{total area of catechin and epicatechin}) + 1$.

2.10 | Toxicity study of SSP in SD rats

Sprague-Dawley rats (150–180 g) were used to determine a long-time adverse effect of SSP. Twenty-four male and female SD rats were purchased from Guangzhou University of Traditional Chinese Medicine. The toxicity study was evaluated as per OECD guidelines. All experiments were approved by the Institutional guidelines of Laboratory Animal Care and Committee on the Use of Live Animals in Teaching and Research (CULATR), School of Basic Medical Sciences, Southern Medical University, Guangzhou, China (CULATR Reference No. HTSW211215). The animals were randomly divided into four groups, with three males and three females per group. SSP was dissolved in water and administered via gavage once a day at doses of 2, 4, 6 g/kg, or water. Their general behavior, signs of toxicity, food intake, and mortality were recorded at an interval of every 2 days. Body weights were recorded at an interval of every 3 or 4 days. After 25 days, the animals were sacrificed by excessive anesthesia. Gross necropsy, calculation of organ index (such as brain, heart, lung, liver, kidney, etc.), pathological examinations of the organs, blood collection, and analysis were performed (Data S3). The experiments were not randomized/blinded. The requirements are considered to be relevant in recent guidelines for best practice of natural products in pharmacological research that has been taken into the account (Heinrich et al., 2020; Izzo et al., 2020).

2.11 | Data analysis

The EC_{50} values and statistical analysis were performed using PRISM 6.0. Data were presented as mean \pm SED or representative of three independent experiments, and significant difference (*) was considered if a p -value of $<.05$ was seen.

3 | RESULTS

3.1 | SSP inhibits SARS-CoV-2 entry

To determine the antiviral activity of SSP, SSP was weighed and dissolved in DMSO to reach a concentration of 40 mg/ml. We previously developed a single-cycle reporter virus pseudotyped with a functional S-glycoprotein of SARS-CoV-2 to capture inhibitors targeting at entry step. As previously described, the pseudoviruses were generated by co-transfection of HEK293T cells with S-glycoprotein expression plasmids and a commonly used HIV backbone vector pNL4-3.Luc. R – E–

(Liang et al., 2013; Liu et al., 2007; Liu et al., 2019; Lu et al., 2012; Yi et al., 2005). To examine the antiviral activity of SSP against SARS-CoV-2, HEK293T-ACE2 cells were then infected with 100 TCID₅₀ SARS-CoV-2 pseudoviruses in the presence of serially diluted SSP. Virus pseudotyped with a second, unrelated viral envelope glycoprotein of VSV-G was included as a control. As shown in Figure 3, SSP displayed an EC₅₀ of 3.5 µg/ml in the inhibition of SARS-CoV-2 pseudovirus infection (Figure 3a) and was devoid of overt cytotoxicity (Figure 3c). No inhibition was observed when SSP was tested against VSV pseudovirus (Figure 3b). Because SARS-CoV-2 and VSV pseudoviruses share the common genetic HIV backbone expressing protease (PR), reverse transcriptase (RT), and integrase (IN), and differ only in their glycoproteins on the surface of the viruses. This result suggested that SSP antagonizes SARS-CoV-2 pseudovirus entry rather than post-entry events (e.g., reverse transcription). Moreover, the lack of antiviral activity against VSV also ruled out the possibility that SSP simply inactivates VSV by acting on viral lipids as a disinfectant.

3.2 | SSP acts by blocking the attachment of SARS-CoV-2 spike envelope S protein to entry receptor ACE2

SARS-CoV-2 enters cells in the host through its surface-anchored S-protein. The S protein mediates viral entry through the RBD in the S1 subunit that specifically recognizes ACE2 as its receptor and then fuses

the viral into host membranes through the S2 subunit. Entry inhibitors usually target protein-protein interactions within the viral envelope proteins or between viral envelope proteins and host cells or inhibit protein-lipid interactions. To determine whether SSP acts by targeting SARS-CoV-2 S protein or host cells, we pre-treated pseudovirus and HEK293T-ACE2 cells with serially diluted SSP for 2 hr at 37°C. The viruses and HEK293 T-ACE2 cells were then recovered and subsequently subjected to infect HEK293T-ACE2 or incubated with untreated SARS-CoV-2 pseudovirus (Rapista et al., 2011). As controls, HEK293T-ACE2 cells were infected with SARS-CoV-2 pseudovirus and then treated with gradient diluted SSP immediately or 2-hr post-infection (hpi). As shown in Figure 3d, SSP treatment at 2-hr post-infection showed limited anti-SARS-CoV-2 activity compared with the virus and SSP being added simultaneously. This result confirmed the antiviral entry activity of SSP against SARS-CoV-2. Moreover, pre-treatment of pseudovirus with SSP resulted in increased inhibition activities with the EC₅₀ value of 2.3 µg/ml, suggesting that SSP targets SARS-CoV-2 viral envelop S protein to inhibit SARS-CoV-2 entry. Notably, pre-treatment of target cells with SSP halted SARS-CoV-2 infection with the EC₅₀ value of 2.1 µg/ml, suggesting that SSP also targets cellular components to inhibit SARS-CoV-2 entry.

To determine whether SSP targets ACE2 receptor to block virus entry, RBD binding assay was performed. HEK293T-ACE2 cells were treated with serially diluted SSP for 2 hr at 37°C, washed, and were then incubated with supernatant collected from RBD-PD1 expressing plasmid transfected HEK293T cells or a goat polyclonal antibody

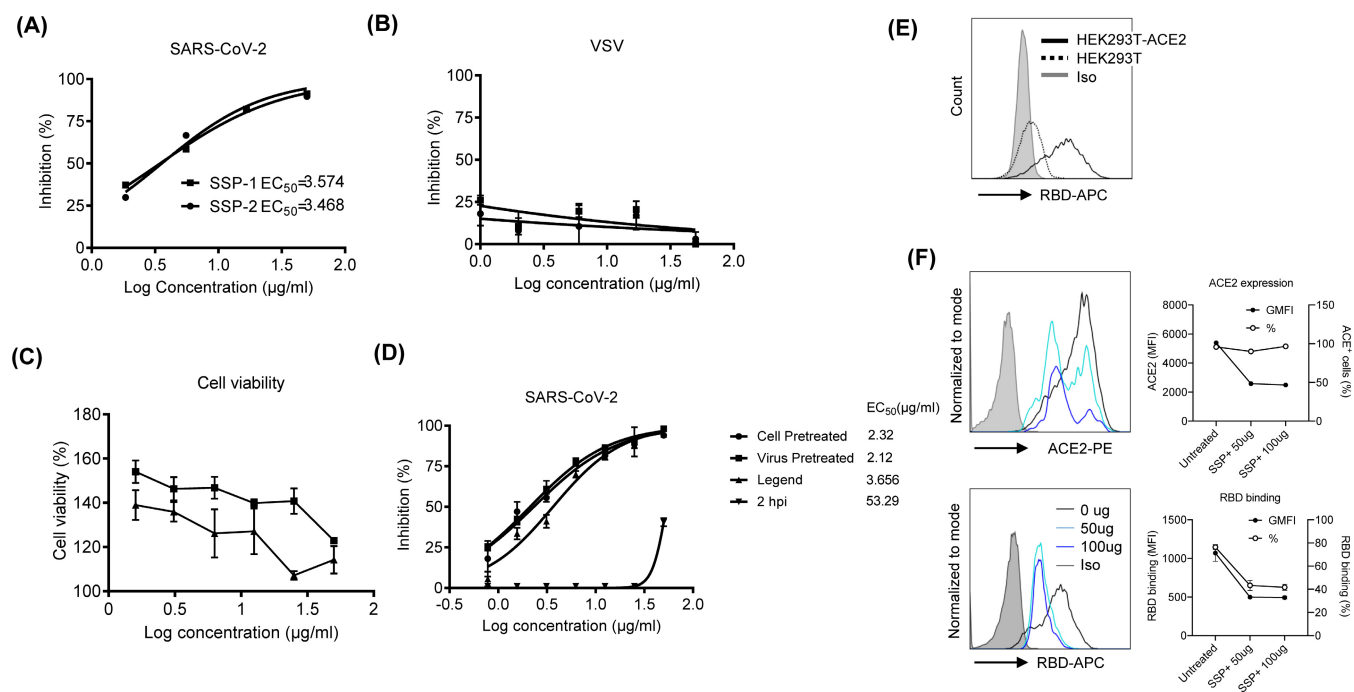


FIGURE 3 Antiviral activity of SSP against SARS-CoV-2. Serially diluted SSP was added to HEK293T-ACE2 cells infected with SARS-CoV-2 (a) and VSV (b) respectively. The luciferase level was measured 2 or 3 days post-infection. To test SSP cytotoxicity, cells viability (c) was measured using the Promega CellTiter-Glo Luminescent Cell Viability Assay kit. (d) Pre-treatment of SARS-CoV-2 and target cells inhibited viral infection. (e) Binding of RBD to ACE2 expressing 293T cells, but not 293T control cells. (f) SSP inhibited RBD binding to target cells. SSP pre-treated HEK293T-ACE2 cells were incubated with RBD-PD1 for 30 mins on ice, followed by antibody staining of ACE2 (upper panel) and RBD (lower panel) and flow cytometry analysis. The data represent the mean ± SEM of triplicate experiments

against ACE2 for 30 min on ice. Cells were then washed and stained with a fluorescent-labeled secondary antibody against goat-IgG or PD-1, respectively. As shown in Figure 3e, untreated HEK293 T-ACE2 cells were positive for both ACE2 and RBD-PD1 staining but negative for the staining of antibodies against goat-IgG and PD-1, which suggested that HEK293T-ACE2 cells had a high expression level of ACE2 and could bind to RBD of SARS-CoV-2 S protein. SSP-treated cells showed significantly reduced geometric mean signal for ACE2 staining but not the percentage of ACE2⁺ cells, suggesting that SSP partially blocked ACE2 specific antibody binding or down-regulated ACE2 expression. In contrast, SSP treatment deducted both geometric mean signal and percentage of positive cells of RBD staining when compared to untreated cells, suggesting that SSP treatment blocked binding of RBD to ACE2 protein (Figure 3f).

3.3 | SSP shows broad-spectrum antiviral activities against SARS-CoV, H5N1, and HIV-1

To determine whether SSP possesses broad-spectrum antiviral activities, a panel of pseudoviruses was generated in our previous studies, including SARS-CoV (L. Liu et al., 2019), H5N1_{Turkey} (Xiao et al., 2013), CCR5-tropic HIV-1_{ADA}, and CXCR4-tropic HIV-1_{HXB2} (Liang et al., 2013), were utilized to test the inhibition rate of SSP. As shown in Figure 4a-d, SSP inhibited infection of SARS-CoV-1, H5N1, and CCR5-tropic HIV-1_{ADA} and CXCR4-tropic HIV-1_{HXB2} with EC₅₀ around 3.64, 5.13, 3.61, and 8.15 µg/ml, respectively, and was devoid of overt cytotoxicity (Figure 4e). This result suggested that SSP has a broad-spectrum antiviral activity against entry of SARS-CoV, H5N1, and HIV-1.

3.4 | SSP blocks SARS-CoV-1 and H5N1 entry by binding to viral envelope and its target cells

To determine whether SSP inhibits viral entry by binding to the SARS-CoV-1 envelope or its receptor on target cells, SSP-virus binding and SSP-cell binding assays were performed. In the SSP-virus binding assay, pseudovirus was initially pre-treated with 50 µg/ml of SSP. The viruses were then recovered by ultracentrifugation and subjected to infect target cells. We found that SSP inhibited SARS-CoV-1 pseudovirus infection at a similar degree when the virus and SSP were added into cells simultaneously (Figure 5). Meantime, the SSP-cell binding assays were performed by pre-treatment of the target cells with SSP for 1 hr at 37°C. After washing by PBS, cells were incubated with SARS-CoV-1 at 37°C for 48 hr (Rapista et al., 2011). We found that pre-treatment of SSP on the target cells inhibited virus infection (Figure 5). The same approach was also used to test the inhibitory effect of SSP against H5N1 with a single high dose of 50 µg/ml. Similar to SARS-CoV-1, SSP treatment on virus particles or their target cells efficiently blocked H5N1 virus entry (Figure 5b).

3.5 | SSP blocks HIV-1 entry by binding to the viral envelope

We tested HIV-1 with a similar but slightly modified experimental protocol by including four anti-HIV drugs: AZT, a potent NRTI, HIV-1 fusion blocker T20, CCR5 antagonist Marvaroc (MVC), and the CXCR4 antagonist JM2987 as positive controls. As shown in Figure 5, AZT, but not SSP, significantly inhibited HIV-1 infection when the treatment was initiated at 2 hr post-infection. In contrast, pre-

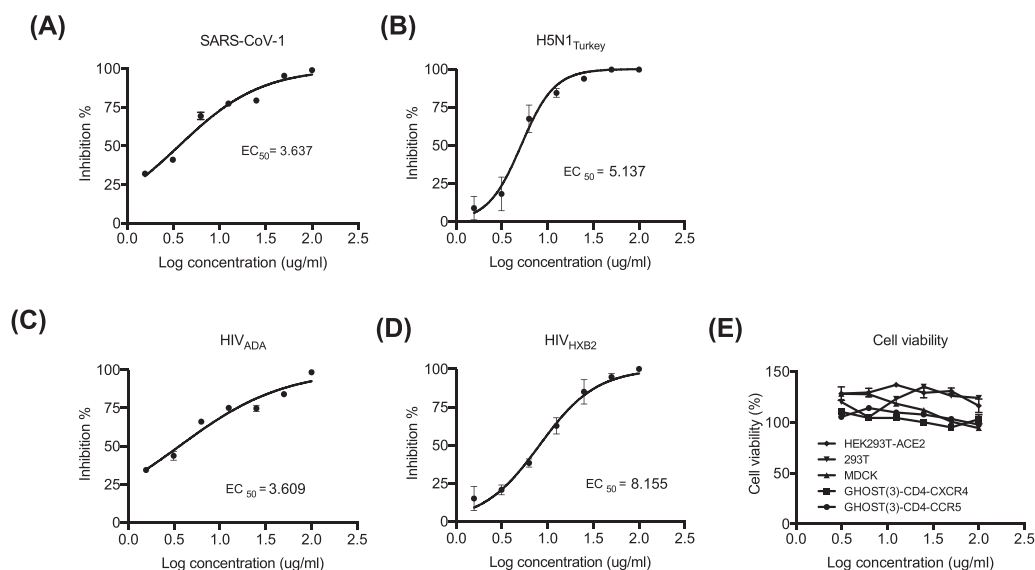


FIGURE 4 Antiviral activity of SSP against SARS-CoV-1, H5N1, and HIV viruses. Serially diluted SSP was added to HEK293T-ACE2, MDCK, GHOST-CCR5, and GHOST-CXCR4 infected with SARS-CoV-1 (a) H5N1 (b) HIV_{ADA} (c), and HIV_{HXB2} (d) respectively. The luciferase level was measured 2 or 3 days post-infection. To test SSP cytotoxicity, cells viability (e) was measured using the Promega CellTiter-Glo Luminescent Cell Viability Assay kit. The data represent the mean ± SEM of triplicate experiments

treatment of the virus with 50 $\mu\text{g}/\text{ml}$ of SSP significantly inhibited HIV-1 infection at a similar degree as T-20, which blocks HIV-1 fusion (Figure 5c–d). Subsequently, the SSP-cell binding assays were performed by treating the target GHOST cells with SSP or with control compounds the CCR5 antagonist Marvaroc (MVC) or the CXCR4 antagonist JM2987 for 2 hr at 37°C. After washing by PBS, cells were subjected to HIV-1_{ADA} or HIV-1_{HXB2} infection and cultivated at 37°C for 48 hr (Rapista et al., 2011). We found that pre-treating the target cells with SSP had no antiviral effect, while MVC and JM2987 showed potent viral inhibition against the respective ADA and HXB2 pseudoviruses at 1 μM as expected (Figures 5e–f). This evidence

demonstrated that SSP inhibited HIV-1 infection by action on the viral envelope glycoprotein gp160, which mediates the viral entry into the host target cells.

3.6 | Antiviral activity of SSP and its effective constituents

To investigate the fractions containing SSP, a feasible UPLC method was used to separate SSP. SSP was divided into three parts, namely Part I, II, and III (Figure 6a). UPLC-ESI-MS/MSn

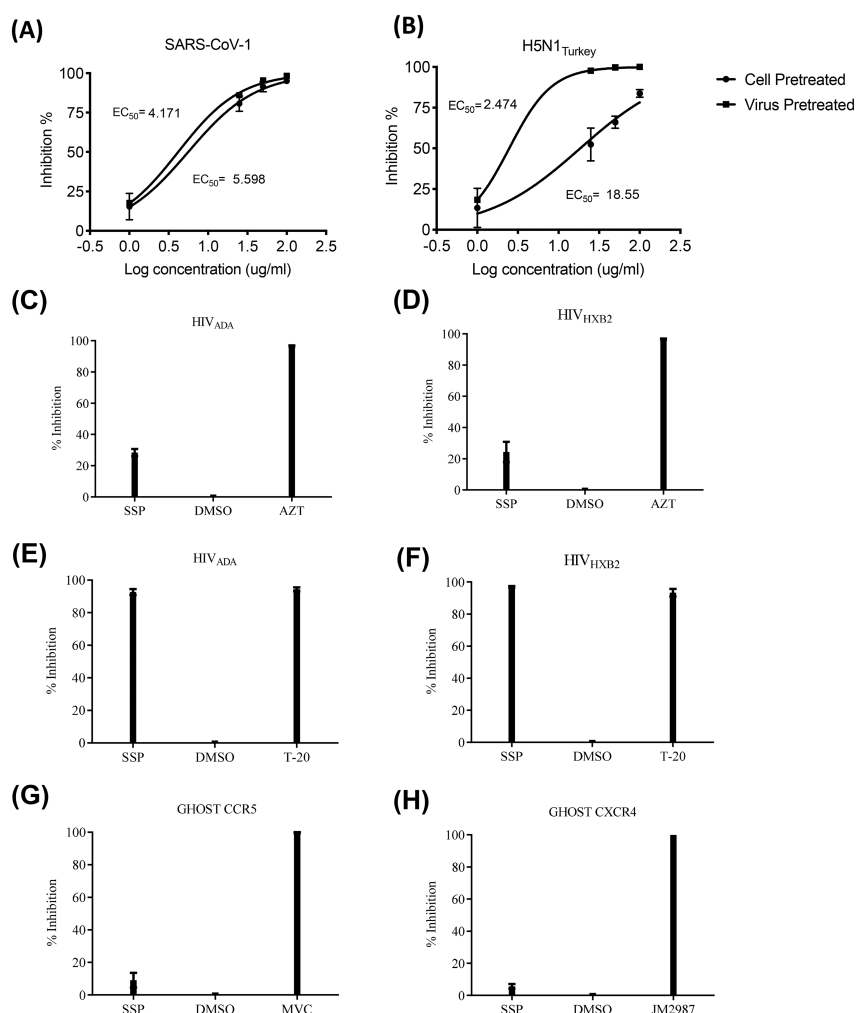


FIGURE 5 Mechanisms of SSP mediated virus entry inhibition. (a ~ b). Pre-treatment of SARS-CoV-1 (a), H5N1 (b) and target cells inhibited viral infection. SARS-CoV-1 or H5N1 pseudovirus and HEK293 T-ACE2 (a) or MDCK (b) cells pre-treated with serial diluted SSP were recovered and subsequently subjected to infect target cells, or incubated with untreated SARS-CoV-1 pseudovirus for 48 hours, respectively. The luciferase level was measured 2 or 3 days post-infection. (c ~ d). Post-entry assay. GHOST-CD4-CCR5 or CXCR4 cells were co-incubated with pseudovirus for 2 hr, washed, and then treated with the presence of 50 mg/ml SSP, dimethyl sulfoxide (DMSO) as the negative control, and 1 mM AZT as a positive control for 48 hr. SSP does not inhibit either HIV-1_{ADA} or HIV_{HXB2} virus gene replication after the viral entry is achieved. (e ~ f). SSP-virus interaction assay. HIV-1_{ADA} and HIV_{HXB2} pseudovirus pre-treated with 50 mg/ml SSP or DMSO as a negative control and entry inhibitor enfuvirtide (T-20) as a positive control. SSP pre-treatment inhibited both HIV_{ADA} and HIV_{HXB2} pseudovirus infection to a similar degree as T-20. (g ~ h) SSP-cell binding assay. GHOST cells were pretreated with SSP or the CCR5 antagonist maraviroc and the CXCR4 antagonist JM2987 as positive controls, and DMSO as a negative control for 1 hr at 37°C prior to being infected with HIV-1_{ADA} or HIV-1_{HXB2}. SSP pretreatment with the cells had no antiviral effect, whereas maraviroc and JM2987 pre-treatment showed strong inhibition against HIV-1_{ADA} and HIV-1_{HXB2} pseudoviruses at 1 mM, as expected. The data represent the mean \pm standard deviation of triplicate experiments

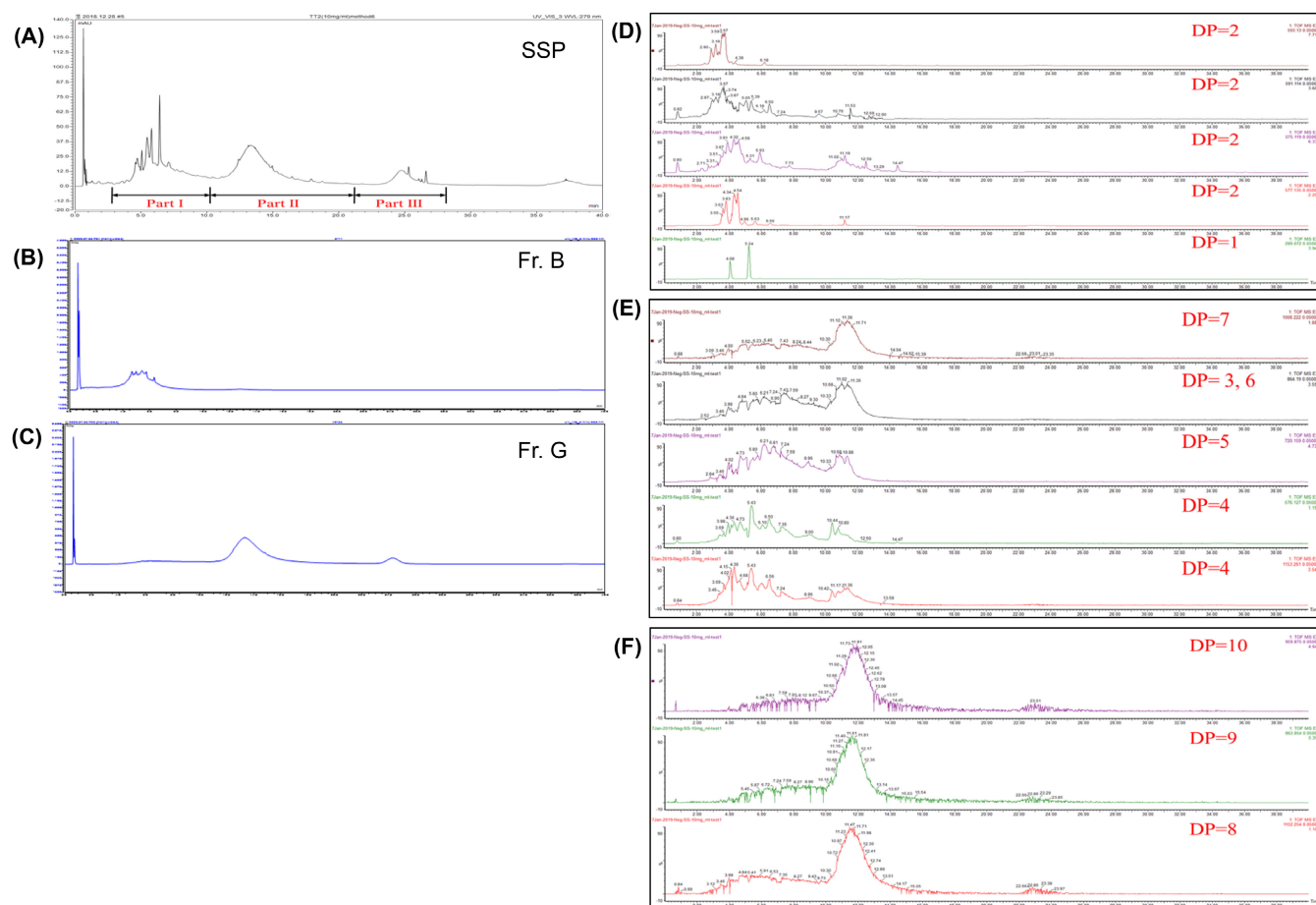


FIGURE 6 Isolation of SSP and UPLC-MS analysis. (a) UPLC-DAD spectra of SSP; (b) UPLC spectra of Fr. B (Part I); (c) UPLC spectra of Fr. G (Part II); (d) Extracted ion chromatogram (EIC) of monomer and dimer of the proanthocyanidins in SSP; (e) Extracted ion chromatogram (EIC) of polymers with mDP between 3 and 7 of the proanthocyanidins in SSP; (f) Extracted ion chromatogram (EIC) of polymers with mDP between 8 and 10 of the proanthocyanidins in SSP

experiment was also performed using the same method (Figure 6d-f), and found that: (a) Monomer and dimer were mainly enriched in the 3–9 min (Part I); (2) 8–10mer were mainly enriched in the 23–33 min (Part II); (3) 3–7mer were both enriched in the two parts. Nevertheless, polymers with a degree of polymerization (DP) above 10 were undetected due to the limited range of molecular weight. Based on this result, different polar solvents were used for the extraction, and the *n*-butanol part (SSP-*n*-BuOH) was selected for further separation by using the macroporous resin columns. Through UPLC's detection, Fr. B and Fr. G were separated into two parts, Part I and Part II, respectively, as mentioned above (Figure 6b-c). In this study, we extracted and greatly enriched proanthocyanidins in SSP, reaching about 60% concentration (Table S6). The thiolysis experiments also proved that the mean degrees of polymerization (mDP) of SSP, SSP-*n*-BuOH, Fr. B, and Fr. G were 3.49, 4.57, 2.95, and 7.52 respectively, which meant macroporous resin columns could effectively separate and obtain parts with different mDPs. Using the method as previously described, we found that SSP, SSP-*n*-BuOH, and Fr. G exhibited lower EC₅₀ in the inhibition of SARS-CoV and SARS-CoV-2 pseudovirus infection than Fr. B (Figure 7a,b). No significant inhibitory

effects on VSV pseudovirus (Figure 7c) or cytotoxicity were observed (Figure 7d). Moreover, pre-treatment of pseudovirus or cells with SSP-*n*-BuOH, Fr. F, or Fr. G inhibited viral entry with lower EC₅₀ value than adding the virus and fragments simultaneously, suggesting that those fragments target both SARS-CoV-2 viral envelop S protein and target cells to inhibit SARS-CoV-2 entry. More importantly, Fr. G exhibited more outstanding bioactivity when compared to Fr. B, suggesting that Part II of SSP contains more effective antiviral activities than Part I. These results revealed that Fr. G contains an intermediate polymer of proanthocyanidins, which may have better antiviral effects.

3.7 | Toxicity study of SSP in vivo

To evaluate the safety of SSP, the cytotoxicity in multiple cell lines was determined by cell toxicity assay (CC₅₀ = 181.2 ~ 339.8 μg/ml as shown in Figure 8a-d). To further examine the toxicity *in vivo*, 24 male and female SD rats were divided into four groups: water (blank control), 2, 4, and 6 g/kg SSP. Drug or water was administered via oral gavage once a day for 25 days. No mortality was observed in any

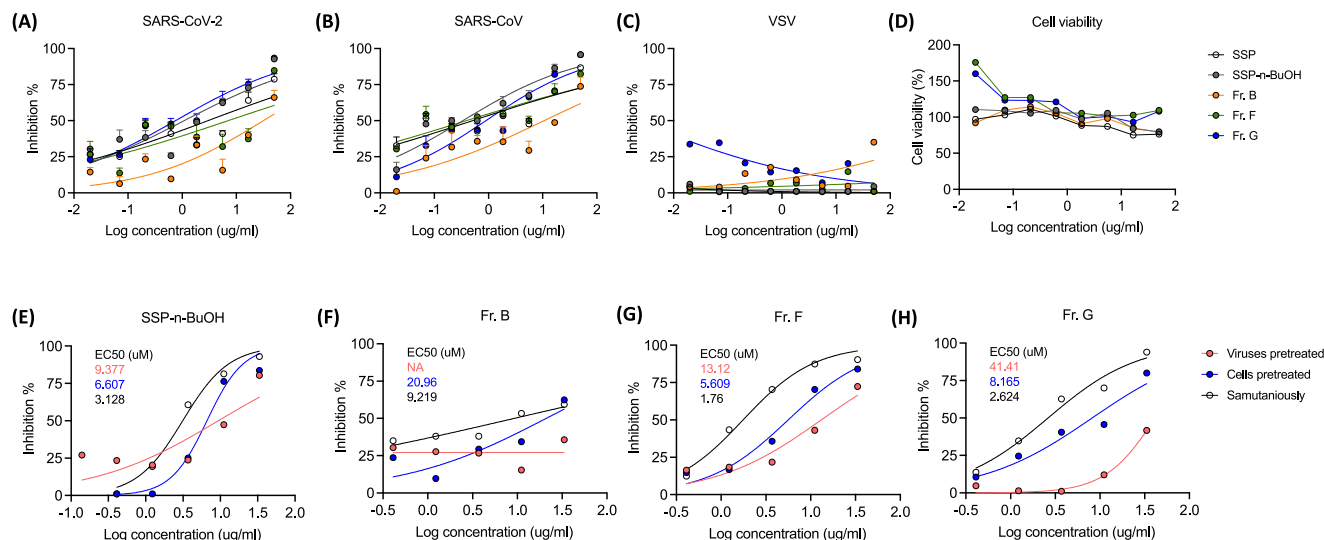


FIGURE 7 Antiviral activity of SSP and their extracted parts against SARS-CoVs, and VSV. As shown in a ~ d, Serially diluted SSP, SSP-n-BuOH, Fr. B, F, and G were added to HEK293T-ACE2 cells infected with SARS-CoV-2 (a), SARS-CoV (b), and VSV (c). The luciferase level was measured 2 or 3 days post-infection. To test their cytotoxicity, cells viability (d) was also measured using the Promega CellTiter-Glo Luminescent Cell Viability Assay kit. (E ~ H) Pre-treatment of SARS-CoV-2 and target cells inhibited viral infection. SARS-CoV-2 pseudovirus and HEK293T-ACE2 pre-treated with serial diluted SSP-n-BuOH (e), Fr. B (f), F (g), and G (h) were recovered and subsequently subjected to infect HEK293T-ACE2, or incubated with untreated SARS-CoV-2 pseudovirus for 48 hr, respectively. As controls, HEK293T-ACE2 cells were infected with SARS-CoV-2 pseudovirus and treated with gradient diluted SSP simultaneously. The data represent the mean \pm SEM of triplicate experiments.

group of rats during the monitoring period (Figure 8). The body weight and food intake were shown in Figure 8e,f. Administration of SSP at the doses of 2, 4, or 6 g/kg to rats did not manifest any signs of toxicity except the loss of body weight in the high dose group. No significant differences in organ indexes (ratio of organ weight to body weight) were observed compared with the control mice (Figure 8g). Levels of glucose, cholesterol, triglyceride, high-density lipoprotein, and low-density lipoprotein were observed normal after SSP administration. No abnormality was observed in levels of blood biochemical parameters such as urea, uric acid, creatine kinase suggesting hepatic, renal, and heart functions were not harmed, indicating that SSP has no apparent toxicity to the experimental rats (Data S3).

4 | DISCUSSION

Over the past two decades, there has been an increased number of viruses causing unexpected illnesses and epidemics among humans. Emerging and re-emerging virus diseases have become a major threat to human and public health. Most of the emerging viruses are of animal origin with RNA genomes and can result in rapid mutation and selection of new variants responding to rapid changes in the relationship between pathogen and host. HIV/AIDS, SARS, and MERS, the outbreak of Ebola virus disease in 2015, and the current pandemic of COVID19 which threatens human health and public safety (Hu et al., 2021). COVID-19, caused by SARS-CoV-2, has affected more than 255 million people worldwide since its emergence in December 2019. The situation is further exacerbated by the potential development of drug-resistant mutants (Zhu

et al., 2020). Hence, there is an urgent need to find broad-spectrum antiviral agents to combat the current COVID-19 pandemic and future emerging viral variants.

SS is one of the most commonly used Traditional Chinese Medicine herbs in the clinical practice of Chinese medicine (Lee et al., 2011; Zhang et al., 2021). A variety of bio-activities concerning antiviral activities have also been revealed. Identification of plant-based bioactive compounds represents great strategies that are cost-effective and potentially used in the management of COVID-19. Several studies show that phytochemicals have a potential role in antiviral properties to combat viral infection and rejuvenate the immune system (Ang et al., 2020; Boozari & Hosseinzadeh, 2021; Idrees, Khan, Memon, & Zhang, 2021; Liskova et al., 2021; Malekmohammad & Rafeian-Kopaei, 2021; Shree et al., 2022). Although not clinically explored yet, the usage of herbal compounds against COVID-19 and other viruses could be a promising approach due to the broad spectrum of their biological activities. The antiviral properties of herbal plants have shed light on the regulation of the viral life cycle, including viral entry, replication, assembly, and release (Ang et al., 2020; Boozari & Hosseinzadeh, 2021; Lin, Hsu, & Lin, 2014).

In the present study, we explored the different fractions of SSP on viral infection using a cell-based assay and single-cycle luciferase reporter on pseudotyped viral envelopes from SARS-CoV-1/2, HIV-1, and influenza A H5N1. The outcome of the study demonstrated that SSP possessed a broad-spectrum antiviral activity against HIV-1, H5N1, and SARS-CoV infection. The main immunogenic components of SARS-CoVs are S-glycoproteins that bind to the host cells' receptors to invade. The human receptor of SARS-CoV-2 is ACE-2, which is intensely expressed on the surface of the alveolar endothelial, brain,

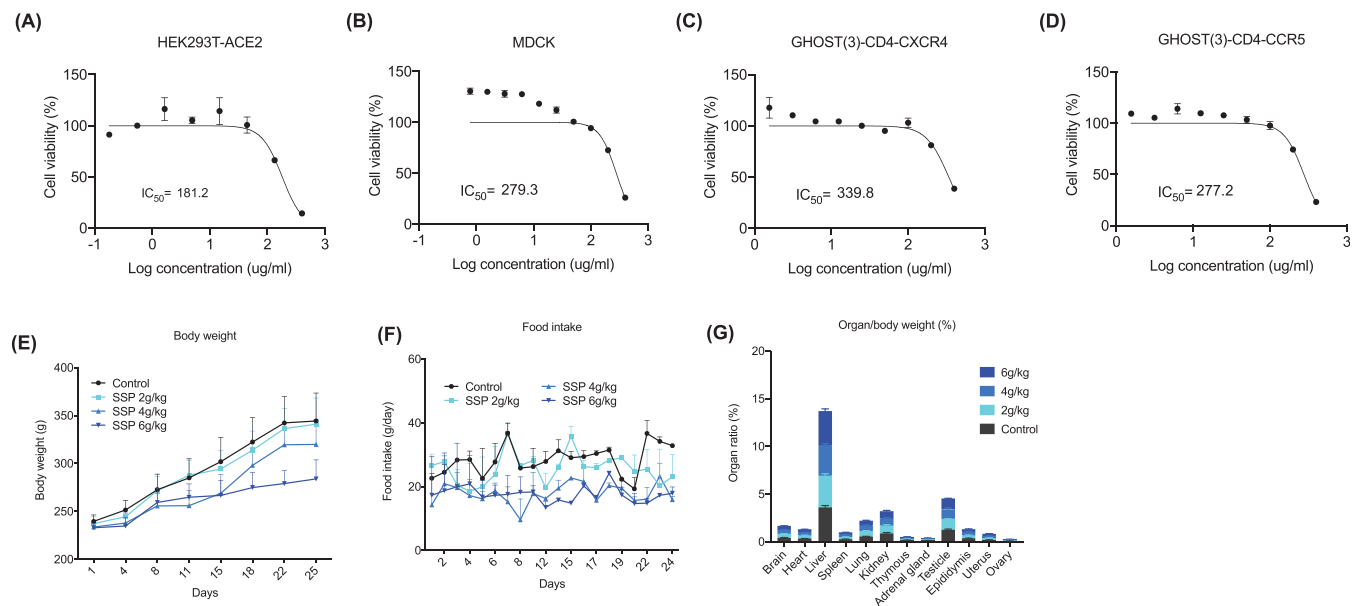


FIGURE 8 SSP did not show significant cytotoxicity in multiple cell lines, or long-term *in vivo* toxicity in rats. (A ~ D) To test SSP cytotoxicity, cells viability was measured in HEK293T-ACE2 (a), MDCK (b), GHOST (3)-CD4-CXCR4 (c) /CCR5 (d). (e) Effects of SSP administration for 4 weeks on the bodyweight of SD rats. (f) Effects of SSP administration for 4 weeks on food intake of SD rats. (g) Effect of SSP administration for 4 weeks on the organ coefficient of SD rats

cardiac, epithelial type II, intestinal, and renal cells and SARS-CoV-2 enters into the cell, releases RNA genome, and replicates (Liskova et al., 2021). When the cell is invaded by the high viral load, the complete protein synthesis mechanism is undertaken to the replication of the virus. Consequently, the assembling of new viral particles leads to exocytosis and apoptotic cell death of the host cell resulting in energetic-metabolic chaos of the virus that spread and infects adjacent cells and organs (Shree et al., 2022).

Our result suggested that SSP antagonizes SARS-CoV-2 pseudo-virus entry rather than post-entry events. Also, SSP blocked the attachment of SARS-CoV S envelope protein on RBD and thereby prevent entry to ACE2 receptor binding. Our results were consistent with earlier studies that phytochemicals inhibit different CoVs targets such as S protein (catechin, genistein, proanthocyanidin A2), dipeptidyl peptidase 4 (epicatechin), a transmembrane serine protease (proanthocyanidin A2), viral enzymes replication such as 3-chymotrypsin-like protease (Iguesterin, quercetin, scutellarin, and myricetin), papain-like protease (cryptotanshinone), helicase (silvestrol), and RNA-dependent RNA polymerase (sotetsuflavone) (Boozari & Hosseinzadeh, 2021; Cherrak, Merzouk, & Mokhtari-Soulimane, 2020; Jena, Kanungo, Nayak, Chainy, & Dandapat, 2021; Liskova et al., 2021; Reddy, GJ, Dodoala, & Koganti, 2021; Zhang et al., 2016), which can be preventive and therapeutic drugs in the combat against CoVs. Our results also suggest that SSP has the potential for treating SARS-CoV diseases and combating new variants of the coronaviruses.

Our result showed that SSP showed broad-spectrum antiviral activities against SARS-CoV-1, H5N1, and HIV-1. Principally, SSP inhibited SARS-CoV-1, H5N1, and HIV-1 entry by binding to the viral envelope and its target cells. The extract of SSP inhibited a very early

stage in the replication cycle, possibly by binding to the virus and preventing entry into the cells. Continued passage of virus in the presence of the extract did not result in the emergence of resistant mutants, in terms of SSP which was tested in parallel. Furthermore, it implicates that SSP inhibited viral entry through a common mechanism of inhibition such as binding to glycan chains of protein in SARS-CoV-1, H5N1, and HIV-1 similar to SARS-CoV-2. These results were consistent with earlier reports that compounds derived from natural products, repress HIV and other viral replication in the host cells (Cary & Peterlin, 2018a; Maria John et al., 2015; Salehi et al., 2018; Wong et al., 2019). Earlier studies have also confirmed that the treatment of SS inhibited HIV type-1 protease activity by about 42.0% at the concentration of 200 μ g/ml. A concentration of 100 μ g/ml of could entirely block both CCR5- and CXCR4-tropic strains of HIV-1 (Lam et al., 2000). Interestingly, SS exhibits potency against replication-competent HIV-1 strains resistant to specific drugs targeting protease (PI) and reverse transcriptase (RT) (Au, Lam, Ng, Fong, & Wan, 2001; Lam et al., 2000). Our findings have also evidenced that SSP is more potent in preventing as specific entry inhibitors.

SARS is caused by SARS-CoV and turned into a pandemic with 37 countries in early 2003 (van Doremalen et al., 2020). Although the disease was successfully contained, SARS-related CoVs still exist in animal host reservoirs, which cause reoccurrence of the outbreak-related disease. Highly pathogenic avian influenza A H5N1, known as bird flu, also infected human and other animal species (Fusade-Boyer et al., 2019), and resulted in about 60% mortality (Kirtipal, Bharadwaj, & Kang, 2020). There is grave concern that H5N1 may mutate and lead to an influenza pandemic among humans (Fusade-Boyer et al., 2019). Currently, only a few drugs are available for

treating H5N1 infection. Oseltamivir, amantadine, and rimantadine are neuraminidase inhibitors that have been practiced to inhibit H5N1 replication and to prevent virus spread between humans (Doshi, Heneghan, & Jefferson, 2016; Jacob et al., 2016). However, generation of oseltamivir, amantadine, and rimantadine resistance H5N1 during treatment was reported (Jacob et al., 2016; Singh & Soliman, 2015). As to SARS-CoV, although some targets for therapeutic prevention have been investigated such as SARS-CoV S-protein, protease, and other proteins concerning the viral life cycle, there are currently no effective vaccines or drugs available for the prevention/treatment of SARS infection (Althwanay et al., 2020).

Blocking of virus entry is a critical strategy for both prevention and treatment (Kang et al., 2012; Kang, Guo, & Chen, 2013). There are only two drugs in this category approved by the FDA for clinical use for HIV in the market: Maraviroc and Enfuvirtide (T-20). Few drugs are available for other emerging diseases. To this end, it is very interesting to discover that SSP can inhibit the viral entry of both CCR5- and CXCR4-tropic HIV-1 ADA and HXB2 strains as well as of H5N1 and SARS-CoV by binding viral envelope glycoproteins directly. Critically, the lack of antiviral effects against VSV rules out the possibility that SSP inactivates VSV by acting like a disinfectant. In support of our findings, several active principles isolated from the plant have also been reported to have some moderate inhibitory ability against HIV-1 entry (Au et al., 2001; Lam et al., 2000). Our results are also consistent with an earlier report that tea polyphenols found in green tea can interrupt membrane fusion between HIV-1 and the host cell plasma membrane (Liu et al., 2005). Further investigations, however, are necessary to reveal the mode of SSP action, which may lead to new drug targets identification on the HIV-1 envelope.

Based on the findings, SSP can be suitable for the prevention and treatment of viral pathogens. The powder SSP was characterized by HPLC spectrum, which was reported in a previous paper from the same lab (Zhang et al., 2021), and further extracted to determine the effective active parts. The Fraction F, G showed better activity than Fraction B, which means the intermediate polymer of PACs may have better antiviral effects. PACs are oligomeric flavonoids rich in SS, which are formed by polymerizing monomeric flavan-3-ols as structural units through C—C bonds and/or C—O—C bonds resulting in condensed tannins (Rauf et al., 2019; Zhang et al., 2016). PACs have attracted more attention due to their significant biological activities, including, antiviral properties (Huang et al., 2012; Kim et al., 2019; Yang et al., 2018). Earlier, studies showed that PACs regulated the immune response by reducing the respiratory syncytial virus-induced proinflammatory cytokines, mucus production, and viral replication in airway epithelial cells (Kim et al., 2019; Lee et al., 2017). Proanthocyanidins from other plants such as *Uncaria tomentosa* and *Reynoutria Rhizome* (Nawrot-Hadzik et al., 2021; Yepes-Perez, Herrera-Calderon, & Quintero-Saumeth, 2022) have been reported to inhibit SARS-Cov-2 virus. In terms of structure activity relationship of proanthocyanidins against the coronaviruses, it was reported that the galloylation and oligomeric types of flavan-3-ols were more likely to inhibit the main protease (M^{pro}) activity of SARS-Cov-2 (Zhu & Xie, 2020). *In vitro* experiments have shown that butanol fractions

enriched with highly polymerized procyanidins displayed effective inhibitory SARS-CoV-2 M^{pro} activity (Nawrot-Hadzik et al., 2021). We, however, found that SSP is a potent SARS-CoV-2 entry inhibitor, which has not been previously reported.

Furthermore, PACs inhibited IL-17-stimulated IL-6 productions in human pulmonary epithelial cells by inhibiting MAPK and NF- κ B-mediated signaling pathways (Kim et al., 2011). PACs and their derivatives can directly target the preS1 region of the hepatitis B virus large surface protein, thereby inhibiting HBV infection (Tsukuda et al., 2017). Zhang et al. (2018) have also reported that PACs A2 could inhibit the replication of porcine reproductive and respiratory syndrome virus *in vitro*. Procyanidin trimer C1 is reported to have synergistic anti-HIV effects when combined with kansui and JQ1 by activating latent HIV (Cary & Peterlin, 2018b). Overall, designing antiviral derivatives from the inspiration of proanthocyanidin compounds are highly promising.

Apart from PACs, SSD comprises many other secondary metabolites in which flavonoids the major bioactive substances, including, (–)-sativan, 3',4',7-trihydroxyflavone, 3'-hydroxy-8-methoxyvestitol, 7,4'-dihydroxy-8-methoxy-isoflavone, blumenol A, butin, calycosin, dihydrokaempferol, dihydrokaempferol, dihydroquercetin, dihydroquercetin, dulcisflavan, eriodictyol, formononetin, formononetin, genistein, glycoside, isoliquiritigenin, liquiritigenin, liquiritigenin, medicarpin, naringenin, plathymenin, prestegane, protocathechuic acid, protocathechuic acid, and prunetin, and many of them exert antiviral properties (Pang et al., 2011; Peng et al., 2019; Peng, Xiong, & Peng, 2020; Tang et al., 2012; Zhang et al., 2021). Some of these major compound(s) is/are accountable for the antiviral efficacy of SSP, which is being investigated in our laboratory. Furthermore, no abnormal toxicity or behavior was detected in long-term SSP treatment in the experimental animals. All the organs and serum biochemical indexes were within the normal range after SSP treatment. Hence, SSP has a broad spectrum of antiviral activities and safe profiles, which warrants treating COVID-19 and other viral infections.

In general, this study is designed to investigate the antiviral activities of SSP on SARS-CoV-2, SARS-CoV-1, HIV-1_{ADA}, HIV-1_{HXB2}, and H5N1. Results indicated that SSP effectively inhibited all these viral envelopes with EC_{50} values ranging from 3.6 to 5.1 μ g/ml. Also, SSP blocked the SARS-CoV-2 S-glycoprotein receptor and host ACE2 receptor domain by binding to its target cells. Proanthocyanidins in SSP can be an active principle that may be a broad-spectrum viral entry inhibitor, in particular, the intermediate polymer of PACs are considered as the primary part with better antiviral effects. SSP not only blocks SARS-CoV-2 infection but also has a broad spectrum of other antiviral activities with safe experimental *in vivo* profiles. Based on the findings, this preclinical study strongly suggests that SSP and its active principles have the complementary to develop into a drug candidate for treating COVID-19 and other emerging enveloped viruses.

ACKNOWLEDGMENTS

This work was partially supported by Guangxi Science and Technology Key Research and Development Program (AB16450012). The authors acknowledge the assistance of Faculty Core Facility, Li Ka Shing Faculty of Medicine, The University of Hong Kong, Hong Kong.

CONFLICTS OF INTEREST

Extraction technology, fractions and their pharmacological activities of SSP is patented by authors: Patent No.CN102462730B, No. CN102579425A, No.IPO0939(HKU), No.63/319,940(HKU). The authors declare no others conflicts of interest concerning this work.

DATA AVAILABILITY STATEMENT

Data available in article supplementary material

ORCID

Kumar Ganesan  <https://orcid.org/0000-0002-3198-6066>

Yibin Feng  <https://orcid.org/0000-0002-0241-670X>

Zhiwei Chen  <https://orcid.org/0000-0002-4511-2888>

Jianping Chen  <https://orcid.org/0000-0001-6494-5271>

REFERENCES

- Althwanay, A., Ahsan, F., Oliveri, F., Goud, H. K., Mehkari, Z., Mohammed, L., ... Rutkofsky, I. H. (2020). Medical education, pre- and post-pandemic era: A review article. *Cureus*, 12(10), e10775. <https://doi.org/10.7759/cureus.10775>
- Andersen, K. G., Rambaut, A., Lipkin, W. I., Holmes, E. C., & Garry, R. F. (2020). The proximal origin of SARS-CoV-2. *Nature Medicine*, 26(4), 450–452. <https://doi.org/10.1038/s41591-020-0820-9>
- Ang, L., Lee, H. W., Kim, A., Lee, J. A., Zhang, J., & Lee, M. S. (2020). Herbal medicine for treatment of children diagnosed with COVID-19: A review of guidelines. *Complementary Therapies in Clinical Practice*, 39, 101174–101174. <https://doi.org/10.1016/j.ctcp.2020.101174>
- Au, T. K., Lam, T. L., Ng, T. B., Fong, W. P., & Wan, D. C. (2001). A comparison of HIV-1 integrase inhibition by aqueous and methanol extracts of Chinese medicinal herbs. *Life Sciences*, 68(14), 1687–1694. [https://doi.org/10.1016/s0024-3205\(01\)00945-6](https://doi.org/10.1016/s0024-3205(01)00945-6)
- Blair, H. A. (2020). Ibalizumab: A review in multidrug-resistant HIV-1 infection. *Drugs*, 80(2), 189–196. <https://doi.org/10.1007/s40265-020-01258-3>
- Boozari, M., & Hosseinzadeh, H. (2021). Natural products for COVID-19 prevention and treatment regarding to previous coronavirus infections and novel studies. *Phytotherapy Research*, 35(2), 864–876. <https://doi.org/10.1002/ptr.6873>
- Cary, D. C., & Peterlin, B. M. (2018a). Natural products and HIV/AIDS. *AIDS Research and Human Retroviruses*, 34(1), 31–38. <https://doi.org/10.1089/aid.2017.0232>
- Cary, D. C., & Peterlin, B. M. (2018b). Procyanidin trimer C1 reactivates latent HIV as a triple combination therapy with kansui and JQ1. *PLoS One*, 13(11), e0208055. <https://doi.org/10.1371/journal.pone.0208055>
- Chan, J. F.-W., Kok, K.-H., Zhu, Z., Chu, H., To, K. K.-W., Yuan, S., & Yuen, K.-Y. (2020). Genomic characterization of the 2019 novel human-pathogenic coronavirus isolated from a patient with atypical pneumonia after visiting Wuhan. *Emerging Microbes & Infections*, 9(1), 221–236. <https://doi.org/10.1080/22221751.2020.1719902>
- Chen, D. H., Luo, X., Yu, M. Y., Zhao, Y. Q., Cheng, Y. F., & Yang, Z. R. (2004). Effect of *Spatholobus suberectus* on the bone marrow cells and related cytokines of mice. *Zhongguo Zhong Yao Za Zhi*, 29(4), 352–355. Retrieved from <https://www.ncbi.nlm.nih.gov/pubmed/15706876>
- Chen, S. R., Wang, A. Q., Lin, L. G., Qiu, H. C., Wang, Y. T., & Wang, Y. (2016). In vitro study on anti-hepatitis C virus activity of *Spatholobus suberectus* Dunn. *Molecules*, 21(10), 1367. <https://doi.org/10.3390/molecules21101367>
- Cheng, X. L., Wan, J. Y., Li, P., & Qi, L. W. (2011). Ultrasonic/microwave assisted extraction and diagnostic ion filtering strategy by liquid chromatography-quadrupole time-of-flight mass spectrometry for rapid characterization of flavonoids in *Spatholobus suberectus*. *Journal of Chromatography. A*, 1218(34), 5774–5786. <https://doi.org/10.1016/j.chroma.2011.06.091>
- Cheng, Y., Fu, Y., Wang, Z., Yang, D., Chen, J., & Wang, D. (2011). Determination on the contents of condensed tannins in *Spatholobus suberectus* Dunn. Extracts and primary study on their anti-tumor activities. *Acta Scientiarum Naturalium Universitatis Sunyatseni*, 50(2), 75–80.
- Cherrak, S. A., Merzouk, H., & Mokhtari-Soulimane, N. (2020). Potential bioactive glycosylated flavonoids as SARS-CoV-2 main protease inhibitors: A molecular docking and simulation studies. *PLoS One*, 15(10), e0240653. <https://doi.org/10.1371/journal.pone.0240653>
- Coutard, B., Valle, C., de Lamballerie, X., Canard, B., Seidah, N. G., & Decroly, E. (2020). The spike glycoprotein of the new coronavirus 2019-nCoV contains a furin-like cleavage site absent in CoV of the same clade. *Antiviral Research*, 176, 104742. <https://doi.org/10.1016/j.antiviral.2020.104742>
- Dong, E., Du, H., & Gardner, L. (2020). An interactive web-based dashboard to track COVID-19 in real time. *The Lancet. Infectious Diseases*, 20(5), 533–534. [https://doi.org/10.1016/S1473-3099\(20\)30120-1](https://doi.org/10.1016/S1473-3099(20)30120-1)
- Doshi, P., Heneghan, C., & Jefferson, T. (2016). Oseltamivir for influenza. *Lancet*, 387(10014), 124. [https://doi.org/10.1016/s0140-6736\(15\)01282-9](https://doi.org/10.1016/s0140-6736(15)01282-9)
- Fehr, A. R., & Perlman, S. (2015). Coronaviruses: An overview of their replication and pathogenesis. *Methods in Molecular Biology*, 1282, 1–23. https://doi.org/10.1007/978-1-4939-2438-7_1
- Fusade-Boyer, M., Pato, P. S., Komlan, M., Dogno, K., Jeevan, T., Rubrum, A., ... Ducatez, M. F. (2019). Evolution of highly pathogenic avian influenza a(H5N1) virus in poultry, Togo, 2018. *Emerging Infectious Diseases*, 25(12), 2287–2289. <https://doi.org/10.3201/eid2512.190054>
- Guo, J. P., Pang, J., Wang, X. W., Shen, Z. Q., Jin, M., & Li, J. W. (2006). In vitro screening of traditionally used medicinal plants in China against enteroviruses. *World Journal of Gastroenterology*, 12(25), 4078–4081. <https://doi.org/10.3748/wjg.v12.i25.4078>
- Heinrich, M., Appendino, G., Efferth, T., Fürst, R., Izzo, A. A., Kayser, O., ... Viljoen, A. (2020). Best practice in research - overcoming common challenges in phytopharmacological research. *Journal of Ethnopharmacology*, 246, 112230. <https://doi.org/10.1016/j.jep.2019.112230>
- Hu, B., Guo, H., Zhou, P., & Shi, Z.-L. (2021). Characteristics of SARS-CoV-2 and COVID-19. *Nature Reviews Microbiology*, 19(3), 141–154. <https://doi.org/10.1038/s41579-020-00459-7>
- Huang, S., Yang, N., Liu, Y., Hu, L., Zhao, J., Gao, J., ... Huang, T. (2012). Grape seed proanthocyanidins inhibit angiogenesis via the down-regulation of both vascular endothelial growth factor and angiopoietin signaling. *Nutrition Research*, 32(7), 530–536. <https://doi.org/10.1016/j.nutres.2012.05.012>
- Idrees, M., Khan, S., Memon, N. H., & Zhang, Z. (2021). Effect of the phytochemical agents against the SARS-CoV and some of them selected for application to COVID-19: A mini-review. *Current Pharmaceutical Biotechnology*, 22(4), 444–450. <https://doi.org/10.2174/1389201021666200703201458>
- Ikeda, T., Tennyson, R. L., Walker, S. N., Harris, R. S., & McNaughton, B. R. (2019). Evolved proteins inhibit entry of enfuvirtide-resistant HIV-1. *ACS Infect Dis*, 5(4), 634–640. <https://doi.org/10.1021/acsinfecdis.8b00362>
- Im, N. K., Lee, S. G., Lee, D. S., Park, P. H., Lee, I. S., & Jeong, G. S. (2014). *Spatholobus suberectus* inhibits osteoclastogenesis and stimulates chondrogenesis. *The American Journal of Chinese Medicine*, 42(5), 1123–1138. <https://doi.org/10.1142/S0192415X14500700>
- Islam, M. T., Sarkar, C., El-Kersh, D. M., Jamaddar, S., Uddin, S. J., Shilpi, J. A., & Mubarak, M. S. (2020). Natural products and their derivatives against coronavirus: A review of the non-clinical and pre-clinical data. *Phytotherapy Research*, 34(10), 2471–2492. <https://doi.org/10.1002/ptr.6700>

- Izzo, A. A., Teixeira, M., Alexander, S. P. H., Cirino, G., Docherty, J. R., George, C. H., ... Ahluwalia, A. (2020). A practical guide for transparent reporting of research on natural products in the British Journal of pharmacology: Reproducibility of natural product research. *British Journal of Pharmacology*, 177(10), 2169–2178. <https://doi.org/10.1111/bph.15054>
- Jacob, A., Sood, R., Chanu Kh, V., Bhatia, S., Khandia, R., Pateriya, A. K., ... Kulkarni, D. D. (2016). Amantadine resistance among highly pathogenic avian influenza viruses (H5N1) isolated from India. *Microbial Pathogenesis*, 91, 35–40. <https://doi.org/10.1016/j.micpath.2015.11.008>
- Jena, A. B., Kanungo, N., Nayak, V., Chainy, G. B. N., & Dandapat, J. (2021). Catechin and curcumin interact with S protein of SARS-CoV2 and ACE2 of human cell membrane: Insights from computational studies. *Scientific Reports*, 11(1), 2043. <https://doi.org/10.1038/s41598-021-81462-7>
- Kang, Y., Guo, J., & Chen, Z. (2013). Closing the door to human immunodeficiency virus. *Protein & Cell*, 4(2), 86–102. <https://doi.org/10.1007/s13238-012-2111-9>
- Kang, Y., Wu, Z., Lau, T. C., Lu, X., Liu, L., Cheung, A. K., ... Chen, Z. (2012). CCR5 antagonist TD-0680 uses a novel mechanism for enhanced potency against HIV-1 entry, cell-mediated infection, and a resistant variant. *The Journal of Biological Chemistry*, 287(20), 16499–16509. <https://doi.org/10.1074/jbc.M112.354084>
- Kim, H., Kim, J. Y., Song, H. S., Park, K. U., Mun, K. C., & Ha, E. (2011). Grape seed proanthocyanidin extract inhibits interleukin-17-induced interleukin-6 production via MAPK pathway in human pulmonary epithelial cells. *Naunyn-Schmiedeberg's Archives of Pharmacology*, 383(6), 555–562. <https://doi.org/10.1007/s00210-011-0633-y>
- Kim, S. J., Lee, J. W., Eun, Y. G., Lee, K. H., Yeo, S. G., & Kim, S. W. (2019). Pretreatment with a grape seed proanthocyanidin extract downregulates proinflammatory cytokine expression in airway epithelial cells infected with respiratory syncytial virus. *Molecular Medicine Reports*, 19(4), 3330–3336. <https://doi.org/10.3892/mmr.2019.9967>
- Kirtipal, N., Bharadwaj, S., & Kang, S. G. (2020). From SARS to SARS-CoV-2, insights on structure, pathogenicity and immunity aspects of pandemic human coronaviruses. *Infection, Genetics and Evolution*, 85, 104502. <https://doi.org/10.1016/j.meegid.2020.104502>
- Lai, K. K., Cheung, N. N., Yang, F., Dai, J., Liu, L., Chen, Z., ... Kao, R. Y. (2015). Identification of novel fusion inhibitors of influenza A virus by chemical genetics. *Journal of Virology*, 90(5), 2690–2701. <https://doi.org/10.1128/jvi.02326-15>
- Lam, T. L., Lam, M. L., Au, T. K., Ip, D. T., Ng, T. B., Fong, W. P., & Wan, D. C. (2000). A comparison of human immunodeficiency virus type-1 protease inhibition activities by the aqueous and methanol extracts of Chinese medicinal herbs. *Life Sciences*, 67(23), 2889–2896. [https://doi.org/10.1016/s0024-3205\(00\)00864-x](https://doi.org/10.1016/s0024-3205(00)00864-x)
- Lee, B. J., Jo, I. Y., Bu, Y., Park, J. W., Maeng, S., Kang, H., ... Lew, J. H. (2011). Antiplatelet effects of *Spatholobus suberectus* via inhibition of the glycoprotein IIb/IIIa receptor. *Journal of Ethnopharmacology*, 134(2), 460–467. <https://doi.org/10.1016/j.jep.2010.12.039>
- Lee, J. W., Kim, Y. I., Im, C. N., Kim, S. W., Kim, S. J., Min, S., ... Chung, N. (2017). Grape seed Proanthocyanidin inhibits mucin synthesis and viral replication by suppression of AP-1 and NF- κ B via p38 MAPKs/JNK signaling pathways in respiratory syncytial virus-infected A549 cells. *Journal of Agricultural and Food Chemistry*, 65(22), 4472–4483. <https://doi.org/10.1021/acs.jafc.7b00923>
- Li, Q., Wu, J., Nie, J., Zhang, L., Hao, H., Liu, S., ... Wang, Y. (2020). The impact of mutations in SARS-CoV-2 spike on viral infectivity and antigenicity. *Cell*, 182(5), 1284–1294. e1289. <https://doi.org/10.1016/j.cell.2020.07.012>
- Li, W., Liu, J., Guan, R., Chen, J., Yang, D., Zhao, Z., & Wang, D. (2015). Chemical characterization of procyanidins from *Spatholobus suberectus* and their antioxidative and anticancer activities. *Journal of Functional Foods*, 12, 468–477. <https://doi.org/10.1016/j.jff.2014.11.009>
- Liang, J., Chen, J., Tan, Z., Peng, J., Zheng, X., Nishiura, K., ... Liu, L. (2013). Extracts of medicinal herb *Sanguisorba officinalis* inhibit the entry of human immunodeficiency virus type one. *Yao Wu Shi Pin Fen Xi*, 21(4), 552–558. <https://doi.org/10.1016/j.jfda.2013.09.034>
- Lin, L. T., Hsu, W. C., & Lin, C. C. (2014). Antiviral natural products and herbal medicines. *Journal of Traditional and Complementary Medicine*, 4(1), 24–35. <https://doi.org/10.4103/2225-4110.124335>
- Liskova, A., Samec, M., Koklesova, L., Samuel, S. M., Zhai, K., Al-Ishaq, R. K., ... Kubatka, P. (2021). Flavonoids against the SARS-CoV-2 induced inflammatory storm. *Biomedicine & Pharmacotherapy = Biomedecine & Pharmacotherapie*, 138, 111430. <https://doi.org/10.1016/j.biopha.2021.111430>
- Liu, L., Fang, Q., Deng, F., Wang, H., Yi, C. E., Ba, L., ... Chen, Z. (2007). Natural mutations in the receptor binding domain of spike glycoprotein determine the reactivity of cross-neutralization between palm civet coronavirus and severe acute respiratory syndrome coronavirus. *Journal of Virology*, 81(9), 4694–4700. <https://doi.org/10.1128/JVI.02389-06>
- Liu, L., Wei, Q., Lin, Q., Fang, J., Wang, H., Kwok, H., ... Chen, Z. (2019). Anti-spike IgG causes severe acute lung injury by skewing macrophage responses during acute SARS-CoV infection. *JCI Insight*, 4(4), e123158. <https://doi.org/10.1172/jci.insight.123158>
- Liu, S., Lu, H., Zhao, Q., He, Y., Niu, J., Debnath, A. K., ... Jiang, S. (2005). Theaflavin derivatives in black tea and catechin derivatives in green tea inhibit HIV-1 entry by targeting gp41. *Biochimica et Biophysica Acta*, 1723(1–3), 270–281. <https://doi.org/10.1016/j.bbagen.2005.02.012>
- Lu, R., Zhao, X., Li, J., Niu, P., Yang, B., Wu, H., ... Tan, W. (2020). Genomic characterisation and epidemiology of 2019 novel coronavirus: Implications for virus origins and receptor binding. *Lancet (London, England)*, 395(10224), 565–574. [https://doi.org/10.1016/S0140-6736\(20\)30251-8](https://doi.org/10.1016/S0140-6736(20)30251-8)
- Lu, X., Liu, L., Zhang, X., Lau, T. C., Tsui, S. K., Kang, Y., ... Chen, Z. (2012). F18, a novel small-molecule nonnucleoside reverse transcriptase inhibitor, inhibits HIV-1 replication using distinct binding motifs as demonstrated by resistance selection and docking analysis. *Antimicrobial Agents and Chemotherapy*, 56(1), 341–351. <https://doi.org/10.1128/AAC.05537-11>
- Reddy, M. P., GJ, H., Dodoala, S., & Koganti, B. (2021). Unravelling high-affinity binding compounds towards transmembrane protease serine 2 enzyme in treating SARS-CoV-2 infection using molecular modelling and docking studies. *European Journal of Pharmacology*, 890, 173688. <https://doi.org/10.1016/j.ejphar.2020.173688>
- Malekmohammad, K., & Rafeian-Kopaei, M. (2021). Mechanistic aspects of medicinal plants and secondary metabolites against severe acute respiratory syndrome coronavirus 2 (SARS-CoV-2). *Current Pharmaceutical Design*, 27(38), 3996–4007. <https://doi.org/10.2174/1381612827666210705160130>
- Maria John, K. M., Enkhtaivan, G., Ayyanar, M., Jin, K., Yeon, J. B., & Kim, D. H. (2015). Screening of ethnic medicinal plants of South India against influenza (H1N1) and their antioxidant activity. *Saudi Journal of Biological Sciences*, 22(2), 191–197. <https://doi.org/10.1016/j.sjbs.2014.09.009>
- Matsuyama, S., Kawase, M., Nao, N., Shirato, K., Ujiike, M., Kamitani, W., ... Fukushi, S. (2020). The inhaled steroid Ciclesonide blocks SARS-CoV-2 RNA replication by targeting the viral replication-transcription complex in cultured cells. *Journal of Virology*, 95(1), e01648-20. <https://doi.org/10.1128/jvi.01648-20>
- Mei, Y., Wei, L., Chai, C., Zou, L., Liu, X., Chen, J., ... Yin, S. (2019). A method to study the distribution patterns for metabolites in xylem and phloem of *Spatholobi caulis*. *Molecules*, 25(1), 167. <https://doi.org/10.3390/molecules25010167>
- Mohammadi Pour, P., Farzaei, M. H., Soleiman Dehkordi, E., Bishayee, A., & Asgary, S. (2021). Therapeutic targets of natural products for the management of cardiovascular symptoms of coronavirus

- disease 2019. *Phytotherapy Research*, 35(10), 5417–5426. <https://doi.org/10.1002/ptr.7172>
- Nawrot-Hadzik, I., Zmudzinski, M., Matkowski, A., Preissner, R., Kesik-Brodacka, M., Hadzik, J., ... Abel, R. (2021). Reynoutria rhizomes as a natural source of SARS-CoV-2 Mpro inhibitors-molecular docking and in vitro study. *Pharmaceuticals (Basel)*, 14(8), 742. <https://doi.org/10.3390/ph14080742>
- Pang, J., Guo, J. P., Jin, M., Chen, Z. Q., Wang, X. W., & Li, J. W. (2011). Antiviral effects of aqueous extract from *Spatholobus suberectus* Dunn. Against coxsackievirus B3 in mice. *Chinese Journal of Integrative Medicine*, 17(10), 764–769. <https://doi.org/10.1007/s11655-011-0642-1>
- Peng, F., Xiong, L., & Peng, C. (2020). (–)-Sativin inhibits tumor development and regulates miR-200c/PD-L1 in triple negative breast cancer cells. *Frontiers in Pharmacology*, 11, 251. <https://doi.org/10.3389/fphar.2020.00251>
- Peng, F., Zhu, H., Meng, C. W., Ren, Y. R., Dai, O., & Xiong, L. (2019). New isoflavanes from *Spatholobus suberectus* and their cytotoxicity against human breast cancer cell lines. *Molecules*, 24(18), 3218. <https://doi.org/10.3390/molecules24183218>
- Qin, S., Wu, L., Wei, K., Liang, Y., Song, Z., Zhou, X., ... Zhang, Z. (2019). A draft genome for *Spatholobus suberectus*. *Scientific Data*, 6(1), 113. <https://doi.org/10.1038/s41597-019-0110-x>
- Rapista, A., Ding, J., Benito, B., Lo, Y. T., Neiditch, M. B., Lu, W., & Chang, T. L. (2011). Human defensins 5 and 6 enhance HIV-1 infectivity through promoting HIV attachment. *Retrovirology*, 8, 45. <https://doi.org/10.1186/1742-4690-8-45>
- Rauf, A., Imran, M., Abu-Izneid, T., lahtisham Ul, H., Patel, S., Pan, X., ... Rasul Suleria, H. A. (2019). Proanthocyanidins: A comprehensive review. *Biomedicine & Pharmacotherapy*, 116, 108999. <https://doi.org/10.1016/j.biopha.2019.108999>
- Richards, K. H., & Clapham, P. R. (2006). Human immunodeficiency viruses: Propagation, quantification, and storage. *Current Protocols in Microbiology*, 15, Unit15J, 11. <https://doi.org/10.1002/9780471729259.mc15j01s02>
- Salehi, B., Kumar, N. V. A., Şener, B., Sharifi-Rad, M., Kılıç, M., Mahady, G. B., ... Sharifi-Rad, J. (2018). Medicinal plants used in the treatment of human immunodeficiency virus. *International Journal of Molecular Sciences*, 19(5), 1459. <https://doi.org/10.3390/ijms19051459>
- Shah, M. A., Rasul, A., Yousaf, R., Haris, M., Faheem, H. I., Hamid, A., ... Batiha, G. E. (2021). Combination of natural antivirals and potent immune invigorators: A natural remedy to combat COVID-19. *Phytotherapy Research*, 35(12), 6530–6551. <https://doi.org/10.1002/ptr.7228>
- Shree, P., Mishra, P., Selvaraj, C., Singh, S. K., Chaube, R., Garg, N., & Tripathi, Y. B. (2022). Targeting COVID-19 (SARS-CoV-2) main protease through active phytochemicals of ayurvedic medicinal plants - *Withania somnifera* (Ashwagandha), *Tinospora cordifolia* (Giloy) and *Ocimum sanctum* (Tulsi) - a molecular docking study. *Journal of Biomolecular Structure & Dynamics*, 40(1), 190–203. <https://doi.org/10.1080/07391102.2020.1810778>
- Singh, A., & Soliman, M. E. (2015). Understanding the cross-resistance of oseltamivir to H1N1 and H5N1 influenza A neuraminidase mutations using multidimensional computational analyses. *Drug Design, Development and Therapy*, 9, 4137–4154. <https://doi.org/10.2147/ddt.S81934>
- Tan, Q., Zhu, Y., Li, J., Chen, Z., Han, G. W., Kufareva, I., ... Wu, B. (2013). Structure of the CCR5 chemokine receptor-HIV entry inhibitor maraviroc complex. *Science*, 341(6152), 1387–1390. <https://doi.org/10.1126/science.1241475>
- Tang, R. N., Qu, X. B., Guan, S. H., Xu, P. P., Shi, Y. Y., & Guo, D. A. (2012). Chemical constituents of *Spatholobus suberectus*. *Chinese Journal of Natural Medicines*, 10(1), 32–35. [https://doi.org/10.1016/s1875-5364\(12\)60007-7](https://doi.org/10.1016/s1875-5364(12)60007-7)
- Tsukuda, S., Watashi, K., Hojima, T., Isogawa, M., Iwamoto, M., Omagari, K., ... Wakita, T. (2017). A new class of hepatitis B and D virus entry inhibitors, proanthocyanidin and its analogs, that directly act on the viral large surface proteins. *Hepatology*, 65(4), 1104–1116. <https://doi.org/10.1002/hep.28952>
- van Doremalen, N., Bushmaker, T., Morris, D. H., Holbrook, M. G., Gamble, A., Williamson, B. N., ... Munster, V. J. (2020). Aerosol and surface stability of SARS-CoV-2 as compared with SARS-CoV-1. *The New England Journal of Medicine*, 382(16), 1564–1567. <https://doi.org/10.1056/NEJMc2004973>
- Wang, Z., Wang, D., Han, S., Wang, N., Mo, F., Loo, T. Y., ... Chen, J. (2013). Bioactivity-guided identification and cell signaling technology to delineate the lactate dehydrogenase A inhibition effects of *Spatholobus suberectus* on breast cancer. *PLoS One*, 8(2), e56631. <https://doi.org/10.1371/journal.pone.0056631>
- Weinreich, D. M., Sivapalasingam, S., Norton, T., Ali, S., Gao, H., Bhoire, R., ... Yancopoulos, G. D. (2021). REGN-COV2, a neutralizing antibody cocktail, in outpatients with Covid-19. *The New England Journal of Medicine*, 384(3), 238–251. <https://doi.org/10.1056/NEJMoa2035002>
- Wong, J. H., Ng, T. B., Wang, H., Cheung, R. C. F., Ng, C. C. W., Ye, X., ... Chan, W. Y. (2019). Antifungal proteins with antiproliferative activity on cancer cells and HIV-1 enzyme inhibitory activity from medicinal plants and medicinal fungi. *Current Protein & Peptide Science*, 20(3), 265–276. <https://doi.org/10.2174/1389203719666180613085704>
- Wrobel, A. G., Benton, D. J., Xu, P., Roustan, C., Martin, S. R., Rosenthal, P. B., ... Gamblin, S. J. (2020). SARS-CoV-2 and bat RaTG13 spike glycoprotein structures inform on virus evolution and furin-cleavage effects. *Nature Structural & Molecular Biology*, 27(8), 763–767. <https://doi.org/10.1038/s41594-020-0468-7>
- Wu, J. T., Leung, K., & Leung, G. M. (2020). Nowcasting and forecasting the potential domestic and international spread of the 2019-nCoV outbreak originating in Wuhan, China: A modelling study. *Lancet*, 395(10225), 689–697. [https://doi.org/10.1016/s0140-6736\(20\)30260-9](https://doi.org/10.1016/s0140-6736(20)30260-9)
- Xiao, H., Liu, L., Zhu, Q., Tan, Z., Yu, W., Tang, X., ... Chen, Z. (2013). A replicating modified vaccinia tiantan strain expressing an avian-derived influenza H5N1 hemagglutinin induce broadly neutralizing antibodies and cross-clade protective immunity in mice. *PLoS One*, 8(12), e83274. <https://doi.org/10.1371/journal.pone.0083274>
- Xu, X., Han, M., Li, T., Sun, W., Wang, D., Fu, B., ... Wei, H. (2020). Effective treatment of severe COVID-19 patients with tocilizumab. *Proceedings of the National Academy of Sciences of the United States of America*, 117(20), 10970–10975. <https://doi.org/10.1073/pnas.2005615117>
- Yang, L., Xian, D., Xiong, X., Lai, R., Song, J., & Zhong, J. (2018). Proanthocyanidins against oxidative stress: From molecular mechanisms to clinical applications. *BioMed Research International*, 2018, 8584136. <https://doi.org/10.1155/2018/8584136>
- Yepes-Perez, A. F., Herrera-Calderon, O., & Quintero-Saumeth, J. (2022). *Uncaria tomentosa* (cat's claw): A promising herbal medicine against SARS-CoV-2/ACE-2 junction and SARS-CoV-2 spike protein based on molecular modeling. *Journal of Biomolecular Structure & Dynamics*, 40(5), 2227–2243. <https://doi.org/10.1080/07391102.2020.1837676>
- Yi, C. E., Ba, L., Zhang, L., Ho, D. D., & Chen, Z. (2005). Single amino acid substitutions in the severe acute respiratory syndrome coronavirus spike glycoprotein determine viral entry and immunogenicity of a major neutralizing domain. *Journal of Virology*, 79(18), 11638–11646. <https://doi.org/10.1128/jvi.79.18.11638-11646.2005>
- Yoon, J. S., Sung, S. H., Park, J. H., & Kim, Y. C. (2004). Flavonoids from *Spatholobus suberectus*. *Archives of Pharmacal Research*, 27(6), 589–592. <https://doi.org/10.1007/BF02980154>

- Zhang, F., Liu, Q., Ganesan, K., Kewu, Z., Shen, J., Gang, F., ... Chen, J. (2021). The Antitriple negative breast cancer efficacy of *Spatholobus suberectus* Dunn on ROS-induced noncanonical Inflammasome Pyroptotic pathway. *Oxidative Medicine and Cellular Longevity*, 2021, 5187569. <https://doi.org/10.1155/2021/5187569>
- Zhang, L., Wang, Y., Li, D., Ho, C. T., Li, J., & Wan, X. (2016). The absorption, distribution, metabolism and excretion of procyanidins. *Food & Function*, 7(3), 1273–1281. <https://doi.org/10.1039/c5fo01244a>
- Zhang, M., Wu, Q., Chen, Y., Duan, M., Tian, G., Deng, X., ... Chen, J. (2018). Inhibition of proanthocyanidin A2 on porcine reproductive and respiratory syndrome virus replication in vitro. *PLoS One*, 13(2), e0193309. <https://doi.org/10.1371/journal.pone.0193309>
- Zhou, S., Hill, C. S., Sarkar, S., Tse, L. V., Woodburn, B. M. D., Schinazi, R. F., ... Swanstrom, R. (2021). β -d-N4-hydroxycytidine inhibits SARS-CoV-2 through lethal mutagenesis but is also mutagenic to mammalian cells. *The Journal of Infectious Diseases*, 224(3), 415–419. <https://doi.org/10.1093/infdis/jiab247>
- Zhu, N., Zhang, D., Wang, W., Li, X., Yang, B., Song, J., ... Tan, W. (2020). A novel coronavirus from patients with pneumonia in China, 2019. *The New England Journal of Medicine*, 382(8), 727–733. <https://doi.org/10.1056/NEJMoa2001017>
- Zhu, Y., & Xie, D. Y. (2020). Docking characterization and in vitro inhibitory activity of Flavan-3-ols and dimeric proanthocyanidins against the Main protease activity of SARS-Cov-2. *Frontiers in Plant Science*, 11, 601316. <https://doi.org/10.3389/fpls.2020.601316>

SUPPORTING INFORMATION

Additional supporting information may be found in the online version of the article at the publisher's website.

How to cite this article: Liu, Q., Kwan, K.-Y., Cao, T., Yan, B., Ganesan, K., Jia, L., Zhang, F., Lim, C., Wu, Y., Feng, Y., Chen, Z., Liu, L., & Chen, J. (2022). Broad-spectrum antiviral activity of *Spatholobus suberectus* Dunn against SARS-CoV-2, SARS-CoV-1, H5N1, and other enveloped viruses. *Phytotherapy Research*, 36(8), 3232–3247. <https://doi.org/10.1002/ptr.7452>